

UNCLASSIFIED

AD NUMBER

AD030443

CLASSIFICATION CHANGES

TO: unclassified

FROM: confidential

LIMITATION CHANGES

TO:

Approved for public release, distribution
unlimited

FROM:

AUTHORITY

NRL ltr. 7103/111, 22 Oct 96; NRL ltr.
7103/111, 22 Oct 96

THIS PAGE IS UNCLASSIFIED

CLASSIFICATION CHANGED

AD

FROM

SECRET

TO

CONFIDENTIAL

3 0 4 4 3

ON

10 OCTOBER 1955

By authority of

List No. 49

Specify Authority Being Used

This action was rendered by

Arthur E Creech OSP

Name in full

Date

Document Service Center, ASTIA

Reproduced

FROM LOW CONTRAST COPY.

AD No. 30443

ASTIA FILE COPY

Hand file

SECRET
SECURITY INFORMATION

NRL Report 4199
COPY NO. 11

SOME THEORETICAL ASPECTS OF THE SONAR GRAPHIC INDICATOR

R. E. Roberson, S. P. Thompson, and H. M. Trent

Applied Mathematics Branch
Mechanics Division

October 12, 1953



NAVAL RESEARCH LABORATORY
Washington, D.C.

SECRET

009934

RECEIVED	
OPNAV	
CENTRAL M	
NOV 6 1953	
REC'D. No.	
COPY No.	71-13
ROUTED TO	

577A-156.38

SECRET

SECURITY

This document contains information affecting the national defense of the United States within the meaning of the Espionage Laws, Title 18, U.S.C., Sections 793 and 794. The transmission or revelation of its contents in any manner to an unauthorized person is prohibited by law.

Reproduction of this document in whole or in part is prohibited except with permission of the issuing office.

SECRET

SECRET

DETACHABLE ABSTRACT CARDS

The abstract cards detached from this document are located as follows:

1. 2.

3. 4.

Signed: Date:

SECRET

SOME THEORETICAL ASPECTS OF THE SONAR GRAPHIC INDICATOR

R. E. Roberson, S. F. Thompson, and H. M. Trent

Applied Mathematics Branch
Mechanics Division

October 12, 1953

NAVAL RESEARCH LABORATORY
Washington, D.C.

SECRET

SECRET

DISTRIBUTION

	Copy No.		Copy No.
OpNav			
Attn: Op-03D	1	Fleet Sonar School, Key West	57-58
Attn: Op-31	2		
Attn: Op-311	3		
Attn: Op-312	4	Fleet Sonar School, San Diego	59-60
Attn: Op-318	5	Attn: LCDR Corbin	61
Attn: Op-34	6		
Attn: Op-32	7	ComOpDevFor	62
Attn: Op-371	8		
Attn: Op-373	9	ComSurASDevDet	63
Attn: Op-374	10		
Attn: Op-42	11	ComHukLant	64-65
Attn: Op-421	12		
Attn: Op-45	13	ComTraComdLant	66
BuShips		ComTraComdPac	67
Attn: Code 565G	14		
Attn: Code 845	15-16	DTMB	68
Attn: Code 846	17		
Attn: Code 848	18	SDC	69
BuOrd		USNSRL	70
Attn: Code Re4b	19-20		
		OCSigO	
ONR		Attn: Ch.Eng. & Tech.Div. SIGET	71
Attn: Code 466	21		
Attn: Code 427	22	SCEL	
Attn: Code 463	23	Attn: SCEL Liaison Office	72-74
Attn: Code 416	24		
		RDB	
USNUSL	25-26	Attn: Technical Library Branch	75-76
USNEL	27-28	Pennsylvania State College	
		Attn: ORL, Navy Representative	77
USNOL	29		
		University of Texas	
USNOTS		Attn: Defence Research Laboratory,	
Attn: Reports Unit	30-31	Dr. C. Paul Boner	78
USNPGS	32	Massachusetts Institute of Technology	
		Attn: Dr. Richard Bolt,	
NATC		Acoustics Laboratory	79
Attn: Electronics Test	33		
NEES	34	Yale University	
		Attn: Prof. L. W. McKeehan	80
NADC	35		
		Columbia University	
WHOI		Attn: Dr. Eugene Booth,	
Attn: Dr. C. O'd Iselin	36	Dobbs Ferry, N. Y.	81
CinC PAC	37	Brown University	
		Attn: Prof. R. B. Lindsay	82
CinC Lant	38		
		Marine Physical Institute	
ComCruDesPac	39	Attn: Dr. Carl Eckart	83
ComDesLant	40	Harvard University	
		Attn: Dr. F. V. Hunt	84
ComSubPac	41-45		
		Scripps Institute of Oceanography	
ComSubLant	46-47	Attn: Roger Ravelle	85
ComSubRon 1	48	Hydrographic Office	86
ComSubRon 4	49-50	National Research Council	
		Attn: Undersea Warfare Comm -	
ComSubRon 6	51-52	John S. Coleman	87-90
ComSub FLOT 1	53-54	Bell Telephone Laboratory,	
		Murray Hill, N. J.	
ComSubDevGru 2	55-56	Attn: Dr. W. Kock	91

SECRET
SECURITY INFORMATION

CONTENTS

Part I
Elementary Aspects

I.1	Introduction.	1
I.2	Basic Concepts	1
I.3	Pattern Formation	2
I.4	Controls	4
I.5	Block Diagram.	4
I.6	Pattern Produced by a Periodic Signal.	5
I.7	Angular Sensitivity.	7
I.8	The SGI as a Doppler Indicator.	8
I.9	The SGI as a Displacement Meter	9
I.10	Concluding Remarks.	10

Part II
The Graphic Indicator as an Antireverberation Device

II.1	Introduction.	11
II.2	Salient Features of the Presentations Due to the Superposition of Two Sinusoids.	13
II.3	The Detection of Echoes Masked by Reverberations	16

Part III
A Model of the Graphic Indicator and its Antinoise Properties

III.1	Introductory Remarks.	22
III.2	A Mathematical Model of the Graphic Indicator	23
III.2.1	Psychology of Visual Perception.	23
III.2.2	Statistical Nature of the Noise Background	25
III.2.3	The Device	26
III.3	Optimization of the Parameters	26

III.4 Summary of Results.	28
III.4.1 Mathematical Results and their Interpretation	28
III.4.2 Results of Immediate Applicability	30
III.4.3 Extension of the Results.	31

Appendixes

I Basic Patterns Produced by a Superposition of Two Sinusoids.	33
II Comparison of Experimental Observations with Theoretical Predictions for Several Cases of the Superposition of Two Sinusoids.	46
III Fundamental Equations in Dimensionless Form	51
IV Optimization with Respect to θ	54
V White Noise	56
VI Six-db Noise	58
VII Notation.	61

ABSTRACT

This report deals with some of the more important theoretical aspects of one of the Navy's newest sonar devices, the Sonar Graphic Indicator.

Emphasis in Part I is upon the visual patterns which are produced by the device in response to a periodic signal, and to the important tactical uses to which these patterns may be put.

Parts II and III concern the device's ability to perform in the presence of reverberations and random noise. Its action in discriminating against reverberations is studied in Part II by considering in detail the patterns which are produced by a superposition of two sinusoids of slightly different frequency.

In Part III is considered the problem of choosing the device's design parameters in such a manner that the operator can best detect a periodic signal in the presence of random noise. Information regarding the optimum values of the bias, bandwidth, and nominal operating frequency is deduced on the basis of plausible, but admittedly assumed, notions about the observer's psychology with respect to visual perception. Particular attention is paid to noise spectrums which are "white," or which fall at 6 db per octave.

PROBLEM STATUS

This report deals with work which was done by the Applied Mathematic Branch as an aid to NRL Problem S07-16. This is an interim report; work is continuing.

AUTHORIZATION

NRL Problem P10-02
RDB Project NF 490-020

Manuscript submitted November 13, 1952

PART I ELEMENTARY ASPECTS

I.1 INTRODUCTION

In the Navy's continuing search for more effective sonar devices, one of the more interesting recent devices is the Sonar Graphic Indicator. With the aid of conferences with the inventors of this device (principally Mr. G. F. Asbury), witnessing of field trials, and certain special studies, the writers of this report have put together a set of explanatory comments which should be of assistance to those who need to understand primarily how this device works rather than how to construct it. Information on the construction of the Sonar Graphic Indicator and on its performance in field evaluation tests is contained in NRL Report No. 4028.*

It appears that the basic problem to be solved in sonar operations is the identification and evaluation of a wanted signal in the presence of disturbing signals. In common parlance, this is known as the "signal-to-noise" problem. Disturbing signals belong broadly to two categories, reverberations and ambient noises. Part II of this report shows how the Sonar Graphic Indicator (hereafter abbreviated as the SGI) is able to find a target echo in the presence of strong reverberations. Part III does the same for ambient noise—which is random in character—and, in addition, gives some hints on how to optimize the design parameters of the device. Part I lays a background for the detailed analyses of Parts II and III and discusses those simple aspects of the SGI that are necessary to understand its operation.

I.2 BASIC CONCEPTS

At the outset, it must be emphasized that the SGI is essentially a nonlinear device. Any attempt to employ conventional linear analyses, or even to use the language of such analyses to too great an extent, can lead only to confusion and poor comprehension of the device. Next, it is important to realize that the device was deliberately designed so that certain statistical quantities associated with the time history of the combined signal plus disturbance are displayed, rather than energy data, as has been done heretofore. More will be said about this later; the important point at the moment is that spectral energy does not play such a dominant role in the operation of the SGI as it does in conventional sonar devices.

The inventors of this device believed that the possibilities of visual displays had not been exploited effectively in prior sonar devices. Eleven attributes of vision have been recognized and described: brightness or lightness, hue, saturation, size, shape, location, flicker, sparkle, transparency, glossiness, and lustre. Some six of these attributes are

*"Sonar Graphic Indicator," by G. F. Asbury, T. O. Dixon, B. G. Hurdle, R. J. Mackey, E. J. Kohn (NRL Report 4028)

used by the SGI in its presentation of information. Generally, the SGI divides the sonar information into a sequence of equal time blocks and presents certain characteristics of each block as a rectangular pattern of light and dark areas on the face of a cathode-ray tube. The presentation of a single block is much like a single television raster; however, there is one fundamental difference. Whereas the moving patterns seen on television, assuming everything is properly synchronized, are easily recognized by the novice, (since, after all, they consist of such well-known items as people, animals, and landscapes), a person looking at an SGI for the first time sees patterns that are totally unfamiliar and hence at the moment seem to be nonsense. Yet it will be clear to him that the moving patterns he sees do have shape, size, location, flicker, brightness, and possibly saturation. As he is trained and acquires more experience, he gradually learns that certain patterns are associated with certain tactical conditions. This kind of knowledge increases until he reaches the stage where most patterns make sense and unusual patterns become a challenge to his interpretative ability. Results to be obtained from such training and experience do not, at the moment, lend themselves to quantitative analysis. The important point is that the eventual possibility of such interpretation was recognized and deliberately built into the SGI, a fact which must be taken into account in any attempt to understand the device.

1.3 PATTERN FORMATION

The formation of patterns on the face of a cathode-ray tube within the SGI will be described in the succeeding paragraphs. Let Figure 1 represent the magnitude-time history of a signal as received by any sonar device. Let us focus our attention on the positive peaks of this signal and say that we are interested in the instants at which these peaks above the dotted line occur, but not in the extent to which they exceed the dotted line. In other words, we are interested in the time of occurrence of any positive peak which exceeds a certain value; we care nothing about negative peaks, about positive peaks less than a certain value, or about actual amplitudes of the larger peaks. The information extracted is simply a set of instants generally irregularly spaced in time. The SGI extracts this information from the signal and displays its time character in the following manner.

Consider a cathode-ray tube with saw-toothed generators applied to the vertical and horizontal deflecting plates. The generator applied to the vertical plates is called the

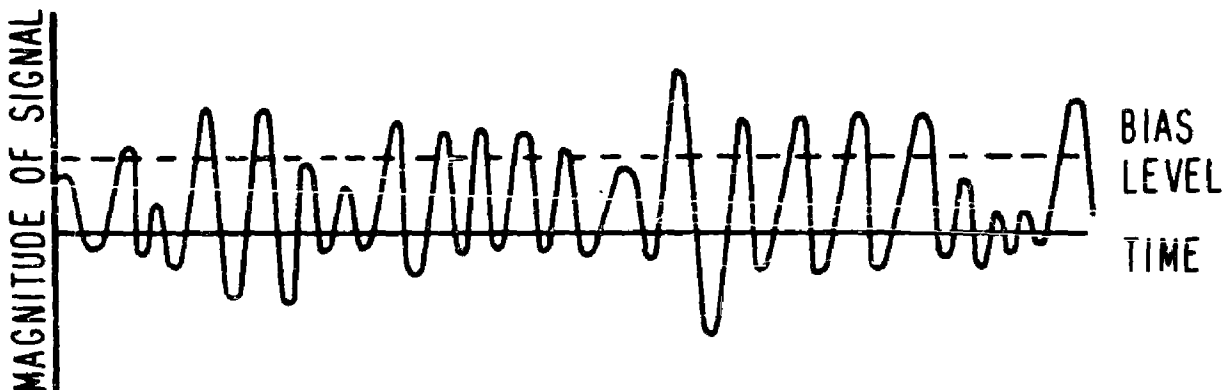


Figure 1 - A sonar signal

"reference oscillator." It causes the beam to be deflected from bottom to top at a uniform rate, followed by a rapid fly-back to the bottom again. Its repetition rate is controllable by the operator and covers a range of, say, 15,000 to 30,000 per second. The generator applied to the horizontal plates is called the "linear time base generator." It sweeps the beam uniformly from left to right, followed by a rapid fly-back. Its repetition rate is also controllable from 2 to 40 per second. The time-base generator establishes the block of information that is seen in one raster. The two generators together specify the position to be occupied by the beam at any instant. At each instant at which a large positive peak occurs in the signal (Figure 1), the intensity grid of the cathode-ray tube is given a positive pulse of voltage, thus producing a bright spot on the face of the tube. The magnitudes of all intensity grid pulses are the same, but the durations can be changed by the operator. He can vary each individual indication from a small dot to an almost vertical line of appreciable extent. Clearly, the position of a spot on the cathode-ray tube is uniquely defined in terms of the original signal and of the two sweep generators.

It is easy to see that if the number of spots produced during one sweep of the horizontal generator is large, the face of the tube will be highly illuminated; if the number is small, the tube will appear dimly illuminated. The face of the tube is never completely dark, for tube and circuit noises alone are bound to produce a few large peaks sufficient to produce spots.

If the spots on the face of the tube occur at completely random instants, the light pattern appearing on the tube will be completely random. At first glance, it would appear that such a pattern would give no information at all. On second thought, however, a perfectly random pattern means that the device is processing perfectly random noise. Such information is not without significance. More interesting patterns occur when the illumination of the face of the tube is not completely random. The operator then recognizes patterns made up of relatively bright and relatively dark areas, which means that positive peaks of the signal do not occur in a completely random fashion and that some degree of regularity has been introduced. Any noticeable regularity at all has some physical significance; and it is the function of the operator, through training and experience, to learn what such patterns mean.

It should be pointed out here that only a very small degree of regularity in a signal is needed to produce a discernable pattern. For example, even a small amount of a-c hum in the circuitry can introduce such a regularity with its characteristic pattern of vertical bands. The meaning of this pattern is soon learned and mentally filed as being of secondary importance. Regularities in a pattern can arise from a myriad of causes, some of which are more important than others. Obviously this report cannot discuss in detail such a large number of possibilities but must be limited to a few which can aid in understanding the device.

Since an operator simply sees a pattern of light and dark areas, it should be apparent that the presence of the dark areas is just as important as the presence of the light areas. It comes as a distinct shock to operators trained on conventional sonar equipments to find that signals are noted in some conditions by the appearance of well-defined dark areas rather than of light ones. It is so easy to assume that an important signal will brighten the face of the tube. This can happen, of course, but the opposite condition is also possible.

1.4 CONTROLS

So far, four controls available to the operator have been indicated. These are: the reference oscillator, the time-base generator, the bias level as illustrated in Figure 1, and the pulse lengthener. The reference oscillator, as the name implies, furnishes a standard against which any regularity in a signal may be compared. As will be explained later, this control changes the appearance of a pattern by changing slopes of characteristic lines in the pattern. The time-base generator allows the operator to expand or contract a pattern in the horizontal direction. The bias level determines the fraction of the positive peaks located in time. Raising the bias level means that few bright spots are produced per second, which tends to reduce the over-all illumination of the tube face. Lowering the bias level does just the opposite and, in fact, tends to saturate the tube face. The pulse lengthener allows the operator to increase or decrease the general level of brightness of the tube with a given rate of spot production. Other controls are best described in terms of a block diagram of the SGI.

1.5 BLOCK DIAGRAM

Figure 2 (which is copied from NRL Report 4028) shows the principal parts of the SGI. The bandpass amplifier is a conventional trf amplifier, except for one thing; it contains a voltage-delayed automatic gain control (AGC) circuit with a time constant of about 0.1 second. The system is able to produce spots with an input of about 0.5 microvolt, and the AGC circuit takes over at about 10.0 microvolts. The AGC circuit is tight, in that a further increase in input signal of 60 db will increase the output only about 3 db. The purpose of the AGC is to present to the pulse generator a signal whose long-time average value is about constant.

The pulse generator contains in its input a voltage-delayed grid-blocking circuit with a rise time of about 0.0015 second, and a decay time which is adjustable from 0.0025 to 0.01 second. This blocking circuit, together with the output control on the amplifier, sets the bias level of the device. This bias level is substantially constant for short periods of time but changes over longer periods, a type of operation that is essential in echo-ranging procedures, where reverberations tend to die out as time proceeds. Any signal accepted by the pulse generator, i.e., one that exceeds the bias level, simply

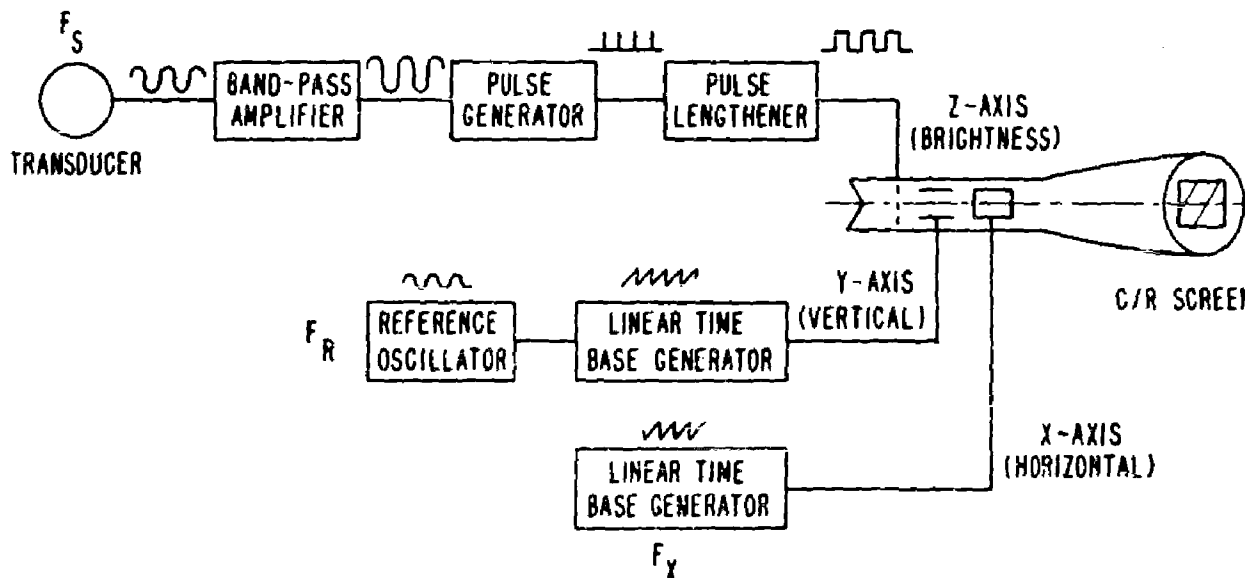


Figure 2 - Sonar Graphic Indicator, simplified

produces a pip as indicated in the drawing. These pips occur in time substantially when positive peaks occur and are applied to the pulse lengthener, which delivers a rectangular pulse of constant height but controllable width each time a pip is applied. It is these rectangular pulses which act on the intensity grid of the cathode-ray tube to produce bright spots. The other parts of the diagram are self-explanatory.

Before leaving the block diagram of the device, it is well to point out that the height of the presentation is determined by the peak voltage delivered by the vertical saw-toothed oscillator, and its width is determined by the horizontal oscillator. Since these values are adjustable, the operator is able to vary his presentation so as to make it pleasing to him. Most operators prefer the presentation to be approximately square. Its area must be small enough so that the operator's eye senses the entire pattern at a glance. This last point is important, since the operator classifies his pattern by comparing all areas of the pattern against one another.

1.6 PATTERN PRODUCED BY A PERIODIC SIGNAL

Since many of the signals to be processed in sonar operations are periodic, the first pattern to be described will be that produced by such a signal. The discussion will be simplified for the moment by assuming that any disturbances are insignificant.

If a periodic signal of period T is presented to the SGI, it will produce a spot of light each time the signal reaches a positive peak. If the gain level is properly adjusted these peaks will occur at equal intervals of time given by

$$t_n = nT - t_0, (t_0 < T), \quad (1)$$

where t_n is the time of occurrence of the n^{th} spot, n is a positive integer, and t_0 allows for the fact that the time origin may not coincide with spot production. The location of the n^{th} spot on the tube face will now be determined.

The vertical position of the electron beam at any instant, t , assuming the origin is at the lower left-hand corner of the pattern, will be given by

$$y = H \left(\frac{t}{T_1} - K_1 \right), \quad 0 \leq \left(\frac{t}{T_1} - K_1 \right) \leq 1, \quad (2)$$

where H is the height of the pattern, T_1 the period of the reference oscillator, and K_1 a positive integer satisfying the inequality shown at the right. K_1 allows for the flyback action of the reference oscillator. In this expression, it is assumed that the time origin is taken when the beam begins a vertical sweep. In a similar fashion, the horizontal or x -position of the electron beam will be given by an expression of the type:

$$x = W \left(\frac{t}{T_2} - K_2 - t_2 \right), \quad t_2 < T_2, \quad 0 \leq \left(\frac{t}{T_2} - K_2 - t_2 \right) \leq 1, \quad (3)$$

where W is the width of the pattern and T_2 is the period of the horizontal time base generator. K_2 plays a similar role to K_1 and t_2 is due to the time origin's not coinciding in general with the start of a horizontal sweep.

Now let it be assumed that

$$T \approx T_1; \quad (4)$$

in other words, that the period of the reference oscillator is near that of the signal. Now at any time, t_n , the vertical position of the spot will be given by

$$y_n = H \left(n \frac{T}{T_1} - \frac{t_o}{T_1} - K_{1n} \right). \quad (5)$$

If n increases by one, then K_1 must increase by one in order to satisfy the conditions of Equation (2). Hence

$$y_{n+1} = H \left(n \frac{T}{T_1} + \frac{T}{T_1} - \frac{t_o}{T_1} - K_{1n} - 1 \right). \quad (6)$$

The change in y from one spot to the next is given by

$$y_{n+1} - y_n = \Delta y = H \left(\frac{T - T_1}{T_1} \right). \quad (7)$$

During the same time interval, K_2 will not, in general, change. Hence

$$x_{n+1} - x_n = \Delta x = W \left(\frac{T}{T_2} \right). \quad (8)$$

These increments of displacement are constant and independent of n . Therefore, the spots lie on a straight line whose slope, S , is given by

$$S = \frac{\Delta y}{\Delta x} = \frac{H}{W} \cdot \frac{T_2}{T_1} \cdot \frac{T - T_1}{T}. \quad (9)$$

Several things can be noted about this relation. In the first place, present models of the SGI have the ratio H/W nearly equal to unity; i.e., the raster is nearly square. Hence this ratio is of minor importance in current designs. Work is under way, however, on other methods of presentation in which W is large compared to H ; but these methods also involve a proportionate increase in T_2 so that the net change in slope is small.

Consider next the ratio T_2/T_1 . This ratio is large compared to unity, being of the order of 3,000, and thus is a significant factor. In fact, the slope can be increased without limit, at least theoretically, by increasing T_2 . Too large a value for T_2 is not desirable in practice, for it is equivalent to a contraction of the pattern in the horizontal direction. It is very easy to reach a condition where nearly every characteristic line in a pattern is nearly vertical, an undesirable operating condition. Finally, the last term shows that the spots can be made to fall on a horizontal line if T_1 , which is under the operator's control, is made equal to T . Furthermore, if T_1 is made smaller than T , the pattern will lie on a straight line with a positive slope. The converse is true if T_1 is greater than T . Typical patterns are shown in Figure 3.

These facts furnish a basis for the easy acquisition of data by an operator. If an SGI receives a periodic signal, then the operator is able to tell instantly from the slope of the pattern whether the period of the received signal is greater or less than that of his reference oscillator. Furthermore, he is able to change his reference oscillator to produce a zero slope in the pattern which automatically matches the period of the reference oscillator to that of the signal.

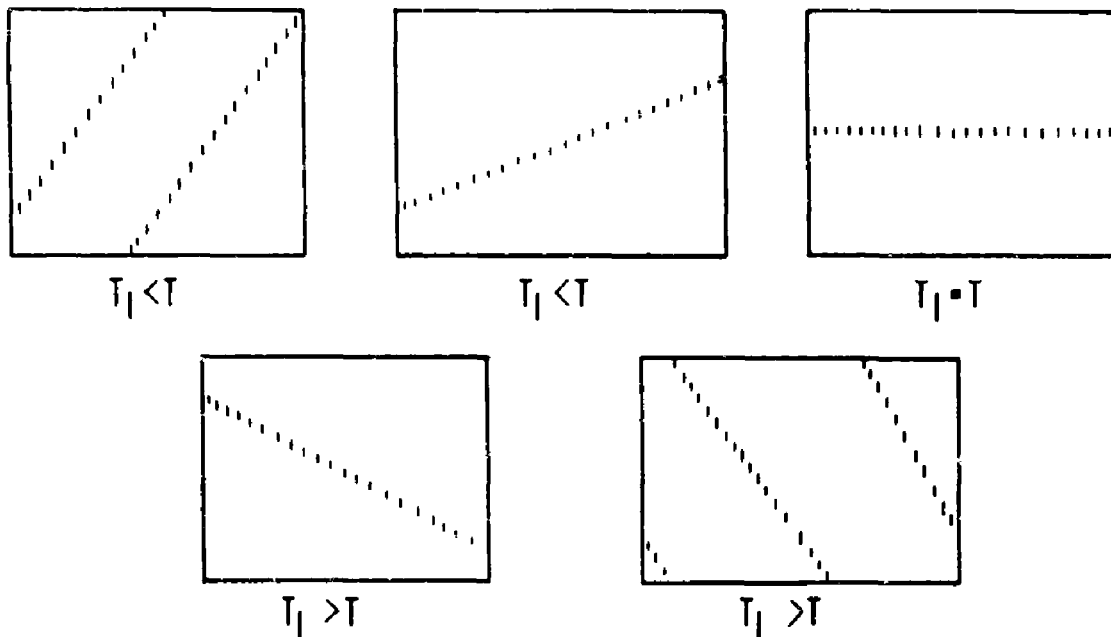


Figure 3 - Typical patterns produced by a sinusoidal signal

1.7 ANGULAR SENSITIVITY

An important property of the SGI is the fact that a small departure of T_1 from T causes a relatively large change in the slope of the pattern. This means, of course, that the device is a very sensitive detector of differences in period. A quantitative expression for this sensitivity will now be found.

If γ is the angle in radians made by the pattern with respect to the horizontal, then, by definition,

$$S = \tan \gamma = \frac{H}{W} \cdot \frac{T_2}{T_1} \cdot \frac{T - T_1}{T}. \quad (10)$$

Let sensitivity be expressed by the change in angle per fractional change in the period of the signal. Then the sensitivity will be given by

$$\text{Sensitivity} = T \frac{d\gamma}{dT} = \frac{H}{W} \cdot \frac{T_2}{T} \cos^2 \gamma. \quad (11)$$

Equation (11) shows that the sensitivity is greatest when the pattern is horizontal ($\gamma = 0^\circ$) and decreases as γ increases. This shows why it is best to keep the reference oscillator adjusted so that the pattern due to the signal forms a horizontal line. It was pointed out previously that H/W is nearly unity and that T_2/T is of the order of 3,000. The real sensitivity can be understood better if angles are expressed in degrees. The appropriate expression is now

$$\text{Sensitivity} = T \frac{d\gamma^\circ}{dT} = \frac{180}{\pi} \cdot \frac{T_2}{T} \cos^2 \gamma. \quad (12)$$

Hence, when $\gamma = 0$ degrees the sensitivity is of the order of 172,000. This means that a

change in the period of the signal of one part in 172,000 will tilt the pattern 1° . Stated another way, a shift in frequency of 1 cps in a 24-kc signal gives a tilt of about 7° . This is sensitivity to an amazing degree.

1.2 THE SGI AS A DOPPLER INDICATOR

The ability of the SGI to indicate small changes in periodicity makes it an excellent instrument for indicating and measuring Doppler effects. Two cases will be considered: the reception of a signal generated by a distant target, and the reception of an echo from a target. In both cases it will be assumed that the medium (water in a sonar application) is at rest, while all targets are in motion.

For the first case, let T be the period of the generated signal, V_o the speed of the receiving vessel along the line to the target, and V_t the speed of the target along the same line and in the same direction. The period of the received signal, T_r , is given by

$$T_r = \frac{c+V_t}{c+V_o} T, \quad (13)$$

where c is the velocity of sound in the medium. Let R be the opening range rate of the target relative to the receiving vessel; i.e., $R = V_t - V_o$. Then the fractional change in period is given by

$$\frac{T_r - T}{T} = \frac{R}{c+V_o} \approx \frac{R}{c}, \quad (14)$$

since $V_o \ll c$. Since the speed of sound in sea water is about 2,880 knots, a range rate of one-tenth knot will produce a fractional change in period of $1/28,800$. With the assumed values used before, this represents a change in angle of a pattern of $172,000/28,800$, or about 6 degrees. This change in tilt of the pattern can be observed by a trained operator.

The case just considered is of importance during pro-submarine operations when the submarine is monitoring the echo-ranging signals of a surface vessel.

For the echo-ranging case, the appropriate relation is

$$T_r = \frac{c-V_o}{c+V_o} \cdot \frac{c+V_t}{c-V_t} T. \quad (15)$$

Introducing again the opening range rate R , it follows that

$$\frac{T_r - T}{T} = \frac{2R}{c} \frac{1}{\left(1 + \frac{V_o}{c}\right)\left(1 - \frac{R+V_o}{c}\right)} \approx \frac{2R}{c}. \quad (16)$$

Comparing Equations (14) and (16) it is seen that the fractional change in period is approximately twice that for a one-way passage of the sound signal. Under the same conditions as used previously, a range rate of one-tenth of a knot will give a change in angle of about 12° . This change in pattern is certainly detectable.

In either case, the fractional change in period is proportional to the range rate. This means that a closing range rate will carry a negative sign and the angular change in the pattern will be negative or clockwise. Since the SGI is so sensitive to changes in range rate, the device has at times been called a Range Rate Indicator.

Equations (14) and (16), which were derived on the basis of a medium at rest, are still valid if the medium is moving at a uniform speed. All that is needed to make the argument hold in this case is to define velocities relative to the medium. The quantity R , being a relative velocity, is an invariant quantity as long as unaccelerated reference coordinates are used.

The foregoing theory is quite general: it assumes only a vehicle carrying an SGI and another target, both of which may move relative to the medium and either of which may be an active source of a periodic signal. Special cases give different applications of the SGI. For example, if the SGI vessels transmit a signal and echoes are received from discontinuities in the medium, then a measure of R gives the speed of the vessel through the water. On the other hand, if the echoes come from the bottom, then a measure of R gives the speed over the ground.

1.9 THE SGI AS A DISPLACEMENT METER

Assume a signal is emitted by a device at point O as shown in Figure 4, and that the



Figure 4 - Motion from P to P'

signal is reflected from a target at P and received at O on an SGI. Assume further that the SGI is adjusted to give a horizontal line pattern. Now let the target be moved from P to P' , a distance X . A positive peak in a transmitted signal will now require more time in transit than previously. The extra time, of course, is $2X/c$, where c is the velocity of the signal. The result on the SGI is to delay the formation of spots by this amount. Since the electron beam of the tube is moving upward across the face of the tube at a speed of H/T_1 , the pattern will be shifted upward a distance $(2H/cT_1)X$. Hence, it is seen that the SGI can serve as a displacement meter since the vertical shift in a pattern is directly proportional to an increase in range of a target. The quantity $2H/cT_1$ can be viewed as an amplification factor. To take some typical sonar values, let $H = 2''$, $T_1 = 1/24,000$ sec, and $c = 4,800$ ft/sec. The constant becomes $5/3$. In other words, the pattern is shifted $5/3$ times as far as the target. Clearly, the target does not have to be shifted far before the pattern is shoved off the top of the raster, but in this case it simply reappears on the bottom.*

The change of a pattern from a horizontal to a sloping line due to a Doppler effect can be viewed from the standpoint of a displacement meter; the actual shift of the pattern

*If the SGI were applied to situations in industrial plants or laboratories where it is desirable to measure small movements of inaccessible surfaces, then the SGI shows real promise. For instance, if the signal had a period of 10^{-6} seconds and was transmitted by air at a velocity of 1,100 ft/sec, then the amplification factor for a 2" raster would be about 305. This is rather good amplification.

upward or downward from one vertical sweep to the next is about $5/3$ of the distance the target moves in a time interval T_1 .

I.10 CONCLUDING REMARKS

In the preceding sections, it has been pointed out that the SGI is essentially a non-linear device that displays the time character of a sequence of instants which represent some of the positive peaks of a signal. The display is in the form of a halftone picture and the ability of an operator, after training and experience, to recognize patterns in the display is basic to the success of the device. The case of a single periodic signal was used to illustrate the fact that patterns are very sensitive to small changes in the time sequence being displayed and that these changes can be measured in a quantitative fashion. Thus a background has been laid for considering the more complex sonar problems of Parts II and III.

PART II

THE GRAPHIC INDICATOR AS AN ANTIREVERBERATION DEVICE

II.1 INTRODUCTION

Our previous attention has been upon the construction of the Graphic Indicator, and upon those of its uses which depend upon its ability to detect minute changes in the frequency of a periodic excitation. We come now to a discussion of its ability to detect and measure the frequency of a signal in the presence of interfering reverberations of slightly different frequency.

Experimentally, it is easily demonstrated that the Graphic Indicator is capable of detecting echoes even when the background reverberations are of only slightly different frequency, and are of much greater intensity - a property whose operational importance is obvious. The problem of providing a full explanation of the reasons for this property is a matter of great complexity.

Fundamentally, this complexity is rooted in the psychophysical nature of the problem. Whereas in sonar equipments of the conventional type one may easily distinguish between the physics and the psychology which are involved, this is not true for the Graphic Indicator. Inasmuch as this is a report about the physics of the device, the explanation which we advance is necessarily incomplete.

Our present purpose is to discuss what is physically present on the cathode-ray screen when the input consists of a signal plus reverberations. In order to provide the reader with perspective with respect to what has experimentally been found important and useful, we shall introduce some notions of a psychological nature. They are admittedly crude in formulation, but are nevertheless useful for descriptive purposes.

Turning our attention to the purely physical portion of the problem, let us consider the nature of reverberations. Experimentally, they appear as a practically continuous "sinusoid," whose amplitude slowly waxes and wanes, and whose frequency slowly but irregularly oscillates about an average value.* Depending upon the frequencies of the horizontal sweep and of the vertical (or reference) sweep, they look on the Graphic Indicator as in Figure 5. The decay of the trace due to the finite persistence of the tube is indicated by dashing the beginning of the line of spots.

Apart from minor wiggles (which by practice one learns to ignore), these traces possess the character which would be expected of a true sinusoid. In particular, the average slope is zero when the average frequency is made equal to the reference frequency, and is nonzero when these frequencies are unequal. As one might suspect, the fact that the reverberations are not sinusoidal is no practical barrier to the determination of their average frequency.

A corresponding situation exists when an echo is superposed upon the reverberations. Although the patterns are, in the fine, essentially more complicated than those due

*Throughout Part II, we shall use "average" in the crude sense of conversational language, rather than as connoting a precisely defined mathematical concept.

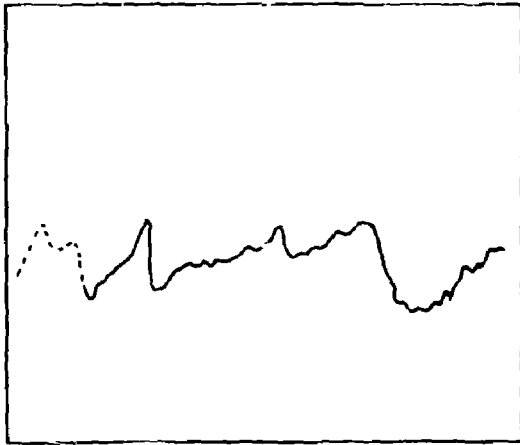


FIG. 5a GI PRESENTATION WHEN
(REFERENCE FREQUENCY) \approx (REVERBERATION
FREQUENCY), AND THE HORIZONTAL SWEEP
IS SET AT A LOW FREQUENCY.

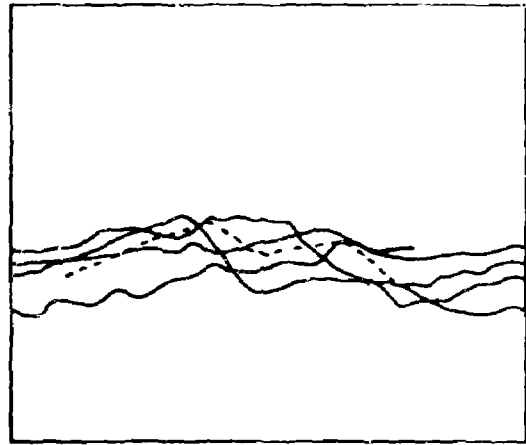


FIG. 5b GI PRESENTATION WHEN
(REFERENCE FREQUENCY) \approx (REVERBERATION
FREQUENCY), AND THE HORIZONTAL SWEEP
IS SET AT A HIGH FREQUENCY.

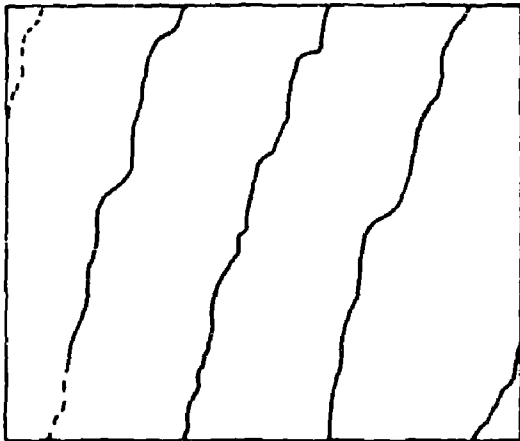


FIG. 5c GI PRESENTATION WHEN
(REFERENCE FREQUENCY) \neq (REVERBERATION
FREQUENCY), AND THE HORIZONTAL SWEEP
IS SET AT A LOW FREQUENCY. (IN THIS
CASE (REFERENCE FREQUENCY) $>$
(REVERBERATION FREQUENCY))

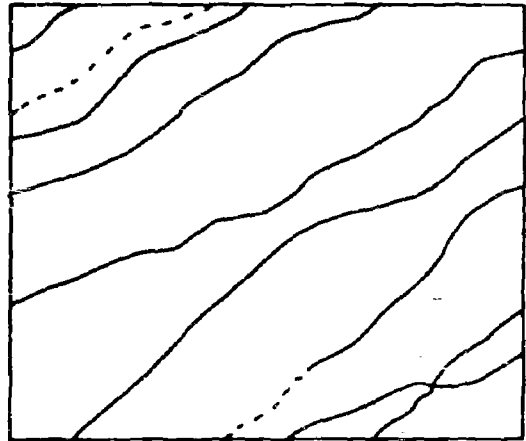


FIG. 5d GI PRESENTATION WHEN
(REFERENCE FREQUENCY) \neq (REVERBERATION
FREQUENCY), AND THE HORIZONTAL SWEEP
IS SET AT A HIGH FREQUENCY. (HERE
ALSO, (REFERENCE FREQUENCY) $>$
(REVERBERATION FREQUENCY))

Figure 5 - Presentations due to reverberations

to a superposition of two sinusoids, the existence of extra wiggles does not significantly alter the observer's impression of the gross appearance. Indeed, by training himself he can learn to ignore the disorder of the wiggles, and be conscious only of the order manifested by the existence of an average slope (and by the existence of other attributes to be subsequently discussed). For these statements there is abundant experimental evidence.

It is accordingly profitless to burden ourselves with a discussion which seeks to reproduce the minor wiggles, and we shall hence draw our conclusions from an analysis of the patterns due to a superposition of two sinusoids. This essentially simpler analysis is quite sufficient to demonstrate all of the pattern attributes used by an operator in recognizing, identifying, and measuring the frequencies of signals; and its ignoring of incoherent irregularities is actually in keeping with the mental response of an experienced observer.

II.2 SALIENT FEATURES OF THE PRESENTATIONS DUE TO THE SUPERPOSITION OF TWO SINUSOIDS

In Appendix I is presented an analysis of the Graphic Indicator patterns which appear when the input consists of the superposition, ξ , of two sinusoids, ξ_1 and ξ_2 :

$$\begin{aligned}\xi &= \xi_1 + \xi_2 \\ \xi_1 &= A_1 \sin(\omega_1 t - \phi_1) , \\ \xi_2 &= A_2 \sin(\omega_2 t - \phi_2) .\end{aligned}\tag{17}$$

For the purposes of this analysis, the action of the automatic gain control (AGC) and of the pulse generator, is presumed to be such that a spot is produced at each instant, t_s , such that the function, ξ , passes through a maximum, i.e., at the instants, t_s , given by:

$$\left(\frac{d\xi}{dt}\right)_{t=t_s} = 0, \quad \left(\frac{d^2\xi}{dt^2}\right)_{t=t_s} < 0 .\tag{18}$$

Since the solutions of Equations (17) and (18) yield the times of occurrence of the spots, and since the position of the electron beam is known as a function of the horizontal and vertical sweep frequencies and the time, the location on the presentation of each spot is, in principle, entirely determined. We shall here discuss only the qualitative results of the calculation, referring the reader to Appendix I for the analytical details.

It turns out that the input, ξ , produces spots as if it were a sinusoid whose frequency slowly varied, and whose phase angle experienced periodic discontinuities. The discontinuities in phase angle produce corresponding discontinuities in the line of spots appearing on the presentation, the latter being accentuated by the AGC action, which prevents the formation of spots at times close to the discontinuities in the phase angle, and hence produces holes in the pattern.

To discuss the patterns which are produced, it is convenient to use ω_1 as the label for the higher circular frequency, so that the frequency ratio, $r = \omega_2 / \omega_1$, is always less than unity,

$$\omega_2 / \omega_1 = r < 1 .\tag{19}$$

In addition to r , the patterns depend upon the ratio, λ , of the maximum slopes of the constituent sinusoids,

$$\lambda \equiv \frac{A_2 \omega_2}{A_1 \omega_1}, 0 < \lambda < \infty. \quad (20)$$

For any specified ω_1 and ω_2 , and any specified values of the vertical and horizontal sweep frequencies, all possible patterns are described by allowing λ to sweep through its indicated range.

If the horizontal sweep is sufficiently slow, the patterns are periodic when the vertical sweep frequency, ω_v , equals either of the constituent frequencies, ω_1 or ω_2 .^{*} When $\omega_v = \omega_1$, one sees a series of curved line segments. The average slope of these line segments is positive, and is small if $\lambda \ll 1$, but is large if $\lambda \gg 1$. When $\omega_v = \omega_2$, the pattern consists of a similar series, but now the average slope of the segments is negative; and is small in magnitude for large λ , but large for small λ .

In both cases, the temporal period of the patterns is $(2\pi/\omega_1 - \omega_2)$ seconds, the spatial period being the product of this with the raster width and the horizontal frequency. This temporal (and hence spatial) period is independent of the value of λ .

In addition to an average slope, the presentations in both cases are characterized by the previously mentioned holes in the patterns. These holes are also periodic with the same period, and they sometimes constitute a feature of the pattern which is easily recognized and which is useful for purposes of identification.

Whether or not the holes are noticeable depends principally upon the initial phase of the vertical sweep frequency, whose influence upon the pattern we may now mention. Since the vertical and horizontal sweeps cause the electron beam to traverse the raster from bottom to top, and then snap back again to the bottom, points at the top of one traversal and at the bottom of the next are substantially coincident in time. Consequently, the fact that some portion of each cycle of the vertical sweep frequency lies at the bottom and top edges of the raster is due solely to the choice of a particular value of the initial phase of the reference frequency. Since this initial phase is subject to the control of the operator, he can choose the top and bottom edges of the pattern at will. An example will illustrate this procedure.

Figure 6a portrays a pattern of oblique lines of spots, upon which, for purposes of reference, we have superposed a dotted horizontal line running through the center of the pattern. If the phase of the vertical sweep is now shifted by π radians, this dotted line will become the top and bottom edges of a new pattern (drawn as Figure 6b), and the top and bottom edges of the old pattern will become the center (marked by a dashed line) of the new pattern. The arrows running from Figure 6a to Figure 6b show how the top, center, and bottom of the old pattern map onto the new pattern. The new pattern has been completed by using the fact that the new lines of spots bear the same vertical relationships to the maps of the top, center, and bottom of the old pattern as did the original lines of spots to the original top, center, and bottom. By repeating the above graphical construction for a sequence of different values of the phase of the reference frequency, we may generate an infinity of different patterns, all of which correspond to the same Graphic Indicator excitation, and to the same vertical and horizontal sweep frequencies. Figure 6c portrays one additional possible construction.

^{*}There are, in addition, other frequency relations which yield periodic patterns. One such will be presented at the end of Part II, and a general discussion will be found in Appendix I. For the antireverberation applications of the Graphic Indicator, the patterns mentioned above in the text are those of principal importance.

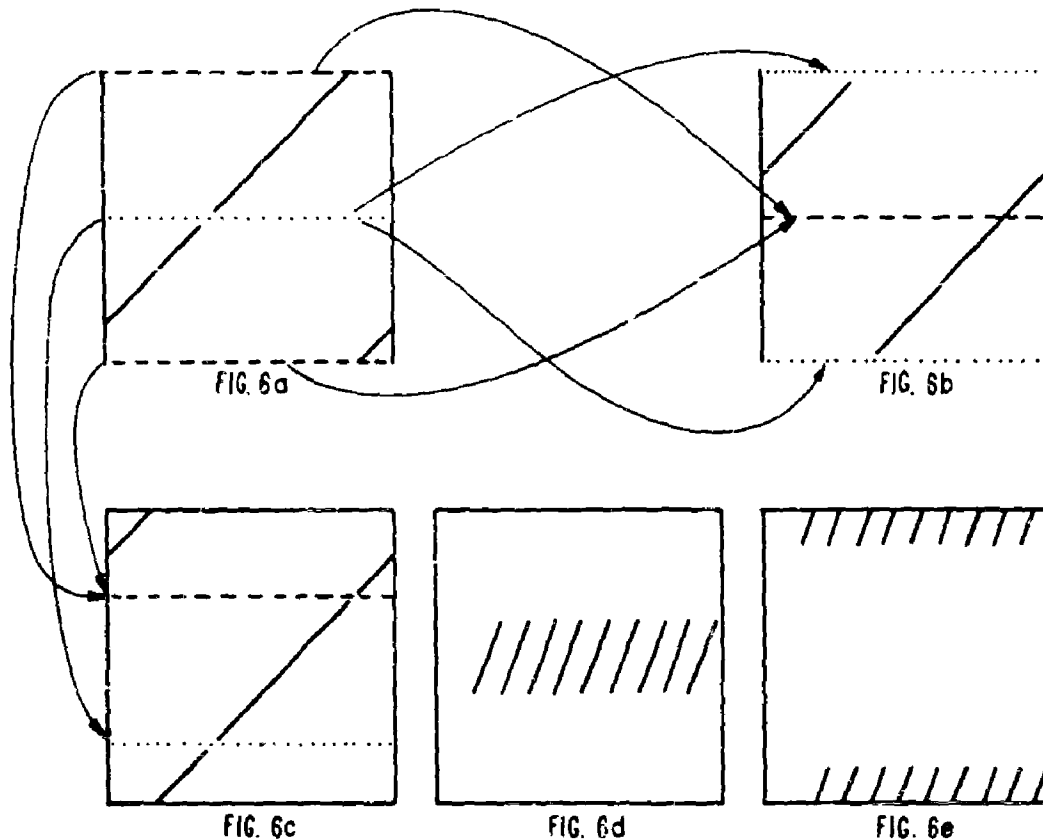


Figure 6 - Effect of change in phase of reference oscillator

Although each of the possible infinity of patterns is experimentally realizable, there is a tendency on the part of an operator to consider only a few of these to be "natural," and to adjust the phase of the vertical sweep so as to realize one of the few which, in his subjective judgment, appear "natural." Most important among the subjective criteria is the requirement of symmetry about a horizontal line through the center of the raster, a condition which is satisfied by Figures 6a and 6b, but not by 6c. Secondly, and almost equally important, the observer tends to center the entity which occupies the least vertical dimension, whether this entity be a hole, or a line segment. For example, when the hole is of slight vertical extent, the observer instinctively prefers Figure 6a to Figure 6b. On the other hand, his choice among the (equivalent) patterns 6d and 6e would almost always be in favor of 6d.*

Drawing upon the results of Appendix I, we have portrayed in Figure 7** the symmetrical patterns (which obey the first subjective criterion of "naturalness") for the case where the vertical sweep frequency is made equal to the higher frequency; the patterns

*The second psychological tendency is materially assisted by a purely physical circumstance which we have ignored in our oversimplified description of the vertical sweep. The fly-back time of the vertical sweep is actually not negligible, but occupies as much as 10% of each cycle. Since the formation of spots is entirely suppressed during each fly-back, the line-segments of Figure 6e are in practice shorter than we have portrayed. If the lines of Figure 6d are sufficiently short, an attempt to produce Figure 6e results, in actuality, in a completely dark screen.

**Figure 7 appears on p. 63

which clearly obey both subjective criteria appear in the top row and are labeled "natural patterns." Corresponding patterns for equality between the lower frequency and the vertical sweep frequency are presented in Figure 8. In each plate, the patterns at the far left are for an input consisting entirely of the frequency which is equal to the vertical sweep frequency, and patterns to the right are for successively greater admixtures with the other frequency, patterns at the extreme right corresponding to an input consisting of a pure sinusoid of the other frequency. Dotted portions of the traces indicate regions where the AGC action suppresses the formation of spots.

The reader should note the similarities and differences between the curves of Figures 7 and 8.* Regardless of whether the vertical sweep frequency equals the higher or the lower frequency, an increasing admixture of the other frequency increasingly tilts and elongates the line segments. As has been previously mentioned, however, the average slope of the line segments is positive in the first case, and negative in the second. These attributes make it possible to decide, in a single ping, whether an echo is of higher or lower frequency than the background reverberations, and to make an estimate of its relative strength.

There remain two matters of practical importance to discuss. First, in forming these periodic patterns, how critical is the adjustment of equality between the vertical sweep frequency and one of the component frequencies? The answer is that it is not critical at all. Indeed, the change in the pattern caused by a small variation in the vertical sweep frequency is almost completely analogous to the corresponding change in the pattern produced by a single sinusoid, namely, a rotation of the entire pattern, including any lines or holes, about the horizontal axis of the presentation. For example, in the case corresponding to Figure 7f, small variations in the vertical sweep frequency produce the changes in the pattern which are portrayed in Figure 9. When the operator is seeking a pattern which he knows to be present, he may (and does) accordingly adjust the vertical sweep frequency as if he were dealing with the straight line due to a single sinusoid, and he quickly learns to judge the extent and sense of the error in any trial adjustment.

Second, how valid are the forms of the foregoing sketches? The answer to this question involves the validity of the psychological notions which have been introduced, and the validity of Appendix I. With respect to our statements about the tendency of observers to attain patterns which are subjectively natural, it should merely be said that they represent the consensus of practiced observers.

Regarding that which is physically present upon the cathode-ray screen, an unequivocal answer can be given. As the reader will see by reference to Appendix II, the agreement between experimental fact and theoretical prediction is, at the very least, adequate. The physical presence of the patterns which have been described is accordingly not open to question.

II.3 THE DETECTION OF ECHOES MASKED BY REVERBERATIONS

Drawing upon our knowledge of the patterns produced by two sinusoids, we may now discuss the operator's procedure in identifying and measuring the frequencies of echoes which are masked by reverberations. This information will be presented in the form of sketches of the patterns which are observed in typical cases.

To remind the reader that the pattern due to the superposition of echo and reverberations is always compared with the pattern due to pure reverberations which exists

Figures 7 and 8 appear on page 63.

(FIGURES ARE DRAWN FOR THE CASE CORRESPONDING TO FIG. 7f)

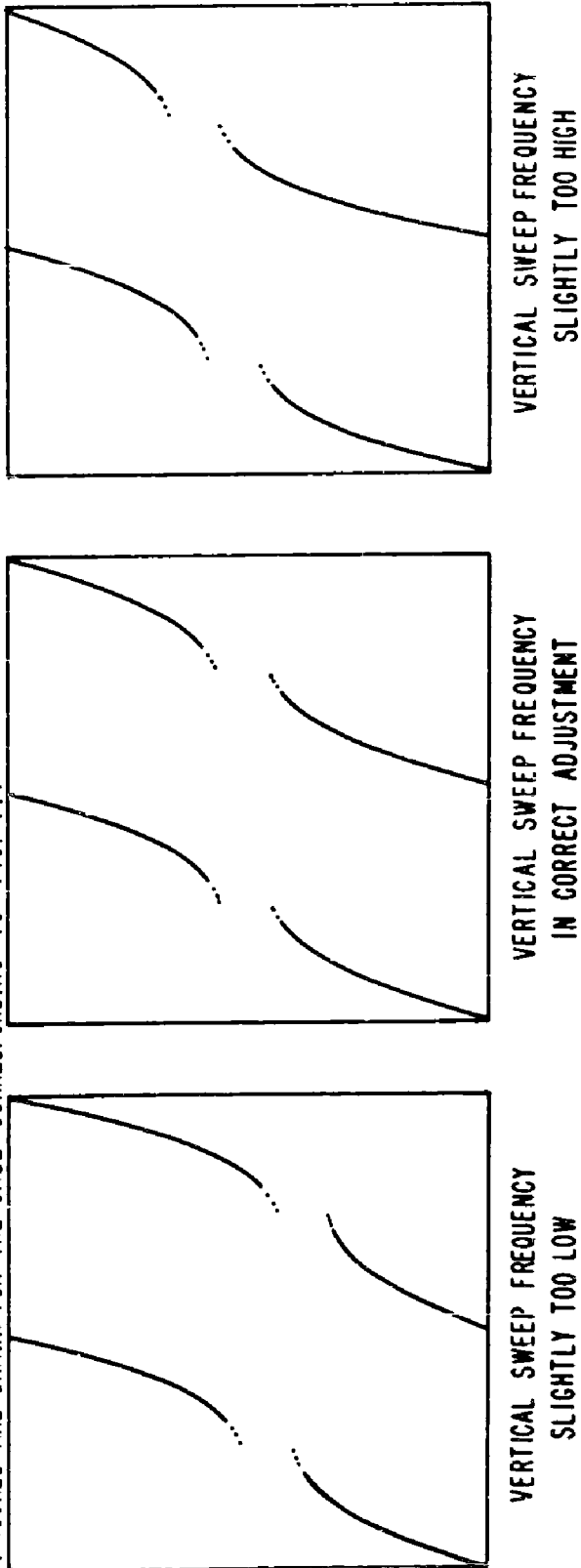


Figure 9 - Effect in a periodic pattern of small variations in the vertical sweep frequency

immediately before and after the echo is received, we shall draw each pattern for several horizontal sweeps of the presentation. To avoid the clutter which results from superposing successive horizontal traversals (as in Figures 5b, 5d), each pattern will be sketched as if the presentation were in the form of a continuous strip instead of a square. As a further simplification in the sketches, the reverberations will be treated as a sinusoid, and the previously discussed similarities and differences between patterns due to reverberations and to a sinusoid should be kept in mind.

The procedure which an operator employs when detecting a new target may be divided into three parts. With the vertical sweep frequency equal to the average frequency of the reverberations, he first observes the screen for the appearance of a pattern characteristic of an echo of different frequency. When such is received, he identifies it as being of higher or lower frequency than the background reverberations, and he forms an estimate of its relative strength; this is the second portion of the procedure. The third and final step is the adjustment of the vertical sweep frequency in the sense indicated by the previous identification of relative frequency. This adjustment is continued, through the period occupied by two or three pings, until the operator recognizes the pattern corresponding to equality between the echo frequency and the vertical sweep frequency.

When a target has already been detected and is being tracked, the above procedure is much shortened. In this case, the operator attempts to maintain equality between the vertical sweep frequency and the echo frequency, so that the reception of each echo results in only a small readjustment. This mode of operation of the Graphic Indicator hence provides a continuous measurement of the target range rate, a measurement which is corrected by each echo separately. This action is in contrast to that of the conventional means of measuring range rate, which requires several pings for its correction.

The previously described steps in the detection and classification of a new target are illustrated in Figures 10 through 13.* In these figures are treated the limiting cases of very strong echoes and very weak echoes. To save space, the corresponding figures for the intermediate cases are omitted, since they differ from those presented only in minor details.

It actually often happens (as, for example, when the range is being closed) that the strength of the echo relative to the reverberations fluctuates from ping to ping, instead of being relatively constant as is implied in the description of procedure just concluded. This state of affairs, while confusing to the uninitiated, is no real handicap to an experienced operator; he concentrates upon making the average slope horizontal, and trains himself to ignore, when necessary, the fact that the average slope is sometimes manifested by the centers of line segments, and sometimes by the centers of holes.

We have discussed the patterns which are observed when the vertical sweep frequency equals either the reverberation frequency or the echo frequency, and we have mentioned the rotation of the pattern which is caused by a slight misadjustment of the vertical sweep frequency. Let us now discuss the appearance of the presentation while the vertical sweep frequency is being lowered (or raised) from the reverberation frequency to the echo frequency.

*As a convention, the duration of the echo in each sketch is taken to be $2[2\pi/(\omega_1 - \omega_2)]$ seconds. In practice, the echo portion of each sketch will, of course, exhibit the number of pattern cycles determined by the duration of the echo.

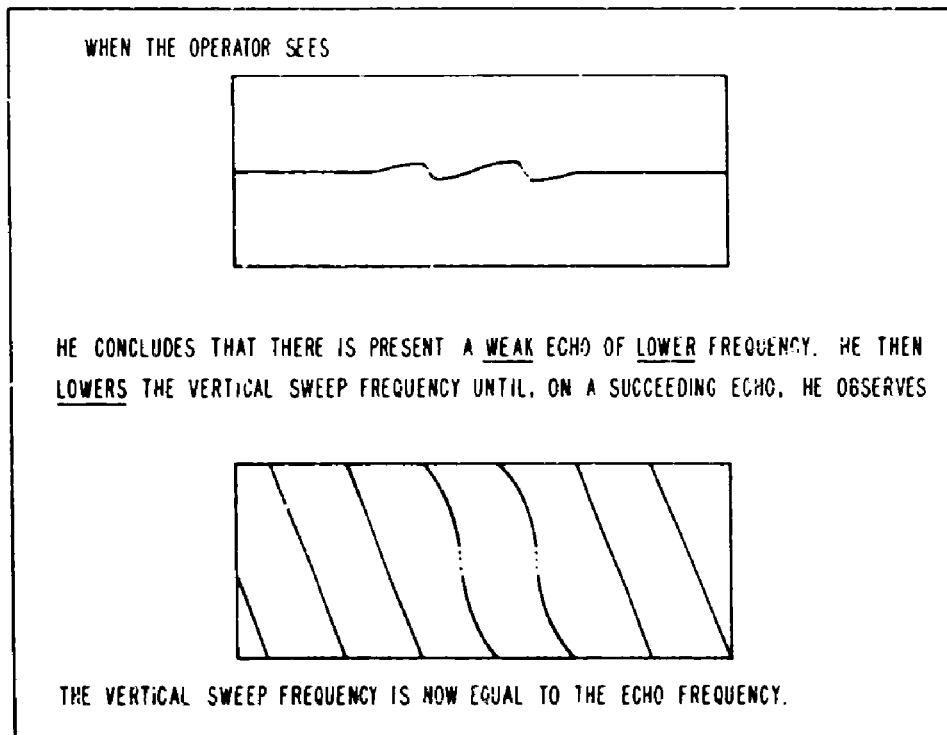


Figure 10 - Procedure for detection and identification of a new target:
weak echo of lower frequency

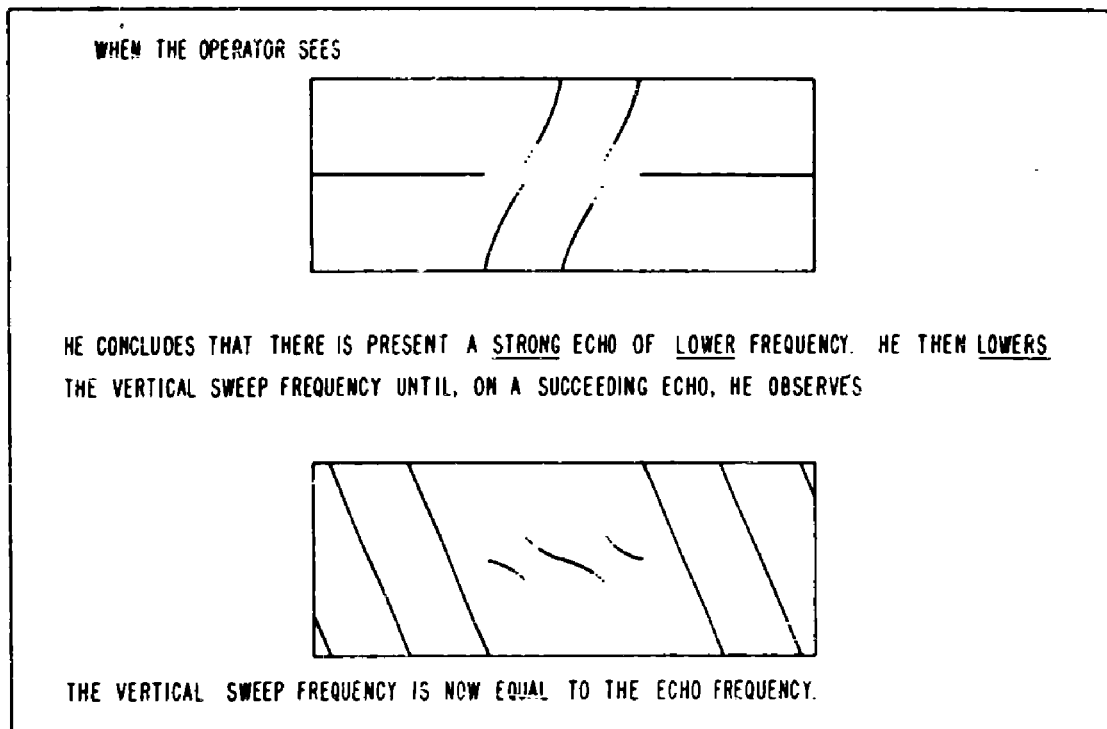


Figure 11 - Procedure for detection and identification of a new target:
strong echo of lower frequency

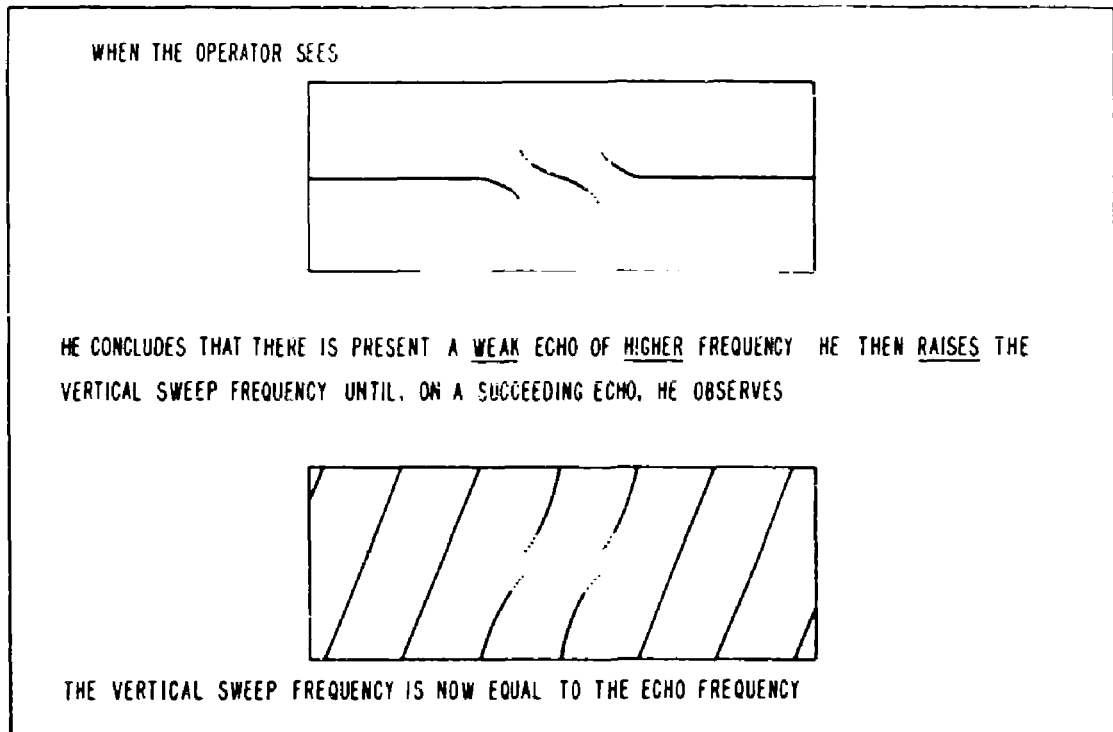


Figure 12 - Procedure for detection and identification of a new target: weak echo of higher frequency

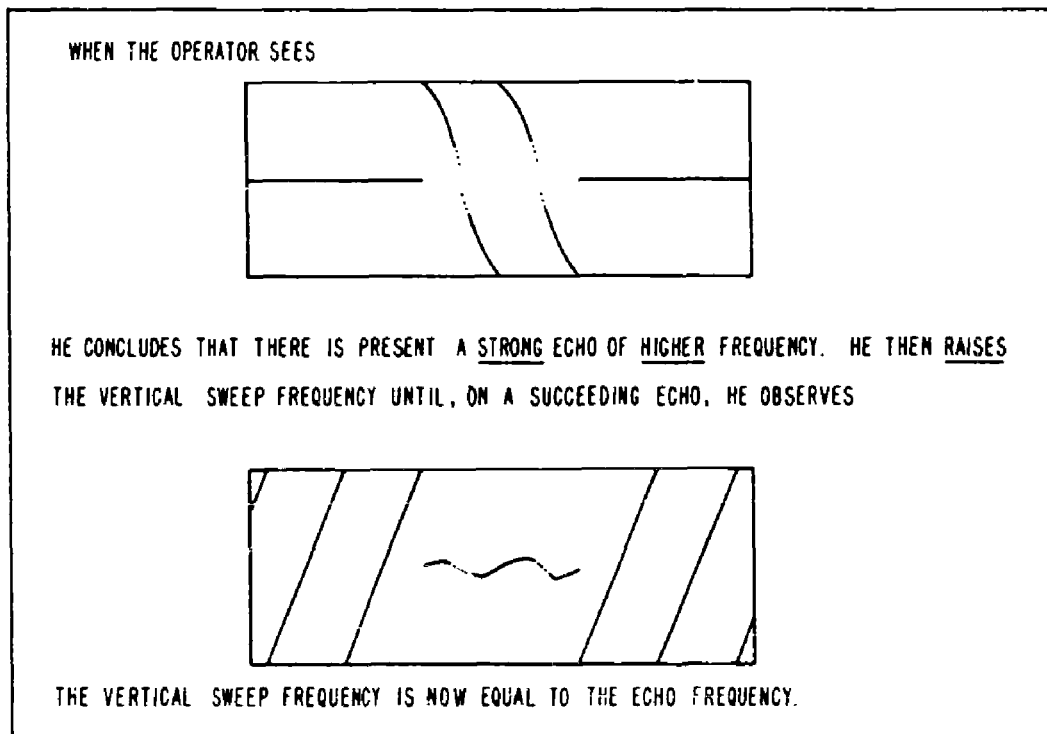


Figure 13 - Procedure for detection and identification of a new target: strong echo of higher frequency

As the vertical sweep frequency is slowly swept through the frequency range, the presentation passes through an infinite sequence of patterns which would be periodic if the horizontal sweep were sufficiently slow. All of these patterns have periods in excess of the period of the patterns which we have previously discussed, and the vast majority of their periods are in excess of the largest practicable period of the horizontal sweep. In consequence, the observed pattern is almost always aperiodic.

In a few cases, the periods are sufficiently short to permit actual observation of the pattern's periodic character. In all cases, however, these periodic patterns are qualitatively different from those which are useful in detecting and identifying echoes, and there is consequently little danger of their becoming confused in the operator's mind. The nature of the qualitative differences can best be presented by an example.

The most easily observed intermediate periodic patterns are those obtained when the vertical sweep frequency is the arithmetic mean of the constituent frequencies. Sketches of these patterns are portrayed in Figure 14 for the cases where the amplitudes are grossly disproportionate. In these patterns it is the double row of holes which makes it easy to distinguish them from the useful patterns which we have discussed previously; similar features distinguish the other intermediate periodic patterns.

Thus, while it is true that the intermediate patterns (both periodic and aperiodic) are full of detail which is confusing to the uninitiated, their existence does not significantly detract from an experienced operator's ability to detect and identify a weak echo.

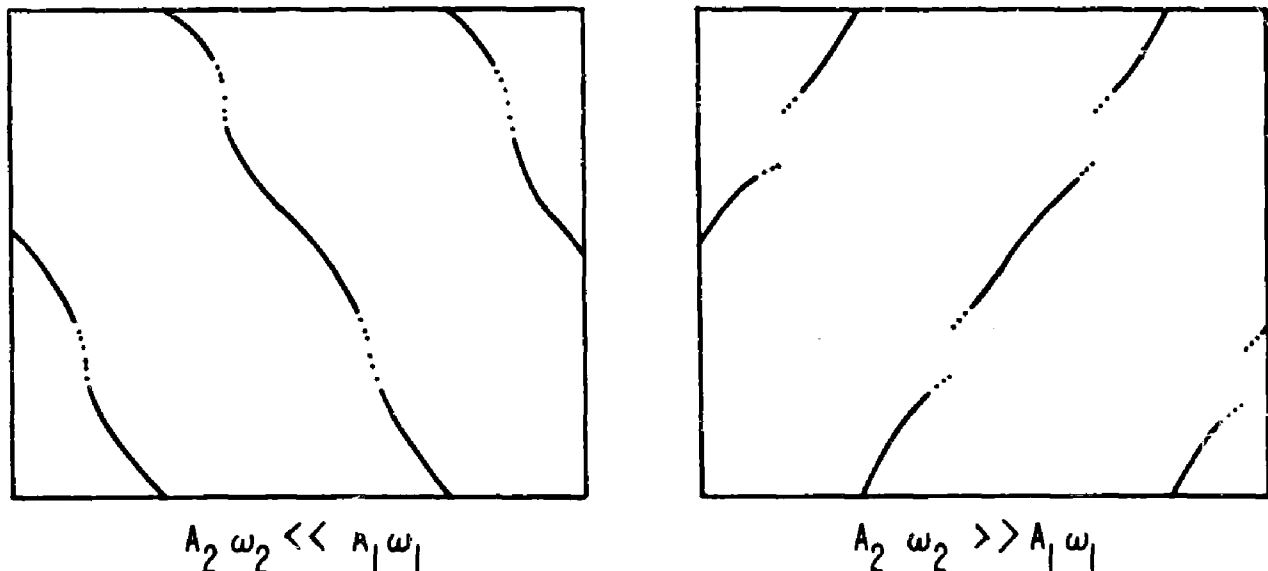


Figure 14 - Patterns obtained when the vertical sweep frequency equals the arithmetic mean of the constituent frequencies

PART III A MODEL OF THE GRAPHIC INDICATOR AND ITS ANTINOISE PROPERTIES

III.1 INTRODUCTORY REMARKS

The operating bias level and the passband of the filter are two of the parameters of the Graphic Indicator with which a designer is concerned. Although the uses which have been discussed in the previous Parts provide some constraint on the permissible ranges of these parameters, there still remains considerable freedom in the choice of specific values. It is clearly desirable to choose values (compatible with these constraints) which give the Graphic Indicator its best antinoise properties. Those values which best enable an operator to detect the presence of a periodic signal when the signal is masked by a noise background will be called the "optimum parameter values" of the device.

The purpose of Part III is twofold: first, to build a mathematical model of the system which includes the Graphic Indicator and its operator; and second, to use this mathematical model in developing a rational basis for choosing optimum values of the design parameters. The optimum values themselves cannot be chosen from purely theoretical considerations. Although the mind of the operator is an essential component of the system, little quantitative information is at present available on the aspects of visual perception which are involved in this device. One may find parameter values which are optimum for a given quantity of a certain kind of visual information. However, to find the amount of the information which is preferred by the average operator, further recourse to experiment will be necessary.

There are two basic steps in the construction of the mathematical model of the system:

- A. Considering the operator as a system component, one must make certain postulates concerning quantities which are believed to be descriptive of the response of the observer's mind to the kind of information presented by the Graphic Indicator.
- B. The nature of the noise background must be postulated. The statistical properties of this noise and the design parameters of the device must be related to the pattern the operator sees presented on the screen.

The optimization problem for the Graphic Indicator as an antinoise device is developed on the basis of this model with three additional steps:

- A. A criterion (hereafter called the "design criterion") is developed for the "goodness" of the design parameters.
- B. Using specific power spectra for the noise background, as much about the general nature of the optimum parameter values is deduced as is possible without a more complete knowledge of the factors of visual perception.

- C. A procedure is outlined for obtaining the experimental information which would be required to extend the optimization results.

III.2 A MATHEMATICAL MODEL OF THE GRAPHIC INDICATOR

To construct a model of the system, the system must first be broken into well-defined components. Each of these must then be abstracted to form a mental picture of a similar component which has all of the essential features of operation of the physical component, but which has been subjected to a process of idealization and simplification in details which do not contribute in a basic way to the functioning of the device. An analogous process to "model construction" in this sense is the production of a pencil sketch or water color. These may convey impressions which are entirely satisfactory representations of the scene yet may omit many details.

A model, to be satisfactory, must explain the essentials of the observed behavior of the physical device. If it is a satisfactory model, its utility is clear. From it, one can predict effects of changing parameters and of introducing auxiliary components in cases where this would be difficult to do freely in the physical device. It must be emphasized that the simplifications inherent in a model of a physical device, provided that the model still explains the behavior of the latter, are usually advantages, rather than handicaps suffered from necessity.

Using the word in a very general sense, there are three major components of the Graphic Indicator. These are: the operator, with his visual and psychological behavior; the world outside the device, which may be sending to it information of a periodic or statistical nature; and the device itself, or "black box," which processes this incoming information and presents it to the operator. The following sections treat these three components sequentially.

III.2.1 Psychology of Visual Perception

Even when the signal-to-noise ratio is remarkably low, it is an experimental fact that an observer may look at the cathode-ray-tube face and correctly decide whether there is a periodic signal superimposed upon the noise background. It is not clear which characteristic of the pattern he sees actually dictates his decision, particularly when his detection ability is being taxed almost to its limit. In the absence of more positive knowledge about the details of visual processes of this kind, one must depend upon the conclusions of those observers who have worked longest with the device. The remarks of this section are the consensus of their beliefs, in the light of such objective evidence as is available.

The mind seems to recognize the degree of average illumination of an entire area, rather than to perceive the geometrical pattern of spots which would be recorded in a snapshot. That is, the mind replaces a group of equally sized and equally illuminated spots by the sensory impression of an equivalent illuminated area. The equivalent area is more or less uniformly illuminated, and overlies the area actually occupied by the configuration of spots. Employing this idea, one is led to discuss the problem of perception of a signal in terms of the problem of distinguishing areas which are of the same size and shape, but which are illuminated to a different degree.

One is not entirely at a loss for quantitative expression in this problem. For many psychological phenomena it has been established that the sensation of difference between

two physical quantities is, for a specified average value of the quantities, proportional to the relative difference between them. It will be assumed that this generally applicable relation holds for the present problem. That is, the ability of an observer to detect a difference between two illuminated areas of equal size is, for a specified average illumination, proportional to the difference in illumination divided by the average illumination.

It remains to relate the question of illumination of areas to the spot pattern actually seen by the observer on the tube face in the presence of noise. From the discussion in Section I.3, it will be seen that areas of greater spot density lie along those lines which would appear if the signal alone were present. Therefore, we may speak of these dense areas, or areas of relatively large equivalent uniform illumination, as corresponding to the peaks of the periodic signal. Conversely, the sparsely spotted areas having low equivalent uniform illumination will be seen to correspond to the valleys of the periodic signal. Equal "light" and "dark" areas on the tube face are represented by equal time intervals about the peaks and valleys of the signal.

Denote by N_T and N_B the rate of crossings of the bias level of the combined signal and noise at the top (or peak) of the signal and at the bottom (or valley) of the signal respectively. Using the assumption that the eye integrates discrete spots into solid areas of illumination, one may take the number of spots falling within an area as a measure of the illumination of that area. From these considerations, the expected relative intensity of illumination of equal areas taken from the regions near the lines of spots and from regions in the darker areas between the lines of spots (which we denote by D) may be written

$$D = \frac{N_T - N_B}{N_T + N_B} \quad (21)$$

Another consideration which affects the operator's ability in visual perception is the over-all illumination intensity of the tube face. The question of whether there exists an optimum absolute level of intensity has not been answered experimentally, but it is the belief of experienced observers that such an optimum level exists. One possible characterization of the over-all background illumination is the total number of spots on the tube face due to noise alone. In turn, this is proportional to the expected number, C , of noise spots occurring in each time-interval equal to the signal period, the signal period being approximately equal to one vertical sweep of the tube face. An alternate interpretation of C is the expected number of crossings of the bias level per signal cycle. Because each spot on the tube face actually occupies a nonzero area, it is possible for a sufficient number of noise crossings per cycle to illuminate the entire tube face (i.e., saturate the tube). Thus, C may sometimes be referred to in terms of "percent saturation" rather than "crossings per cycle."

The considerations of this section have motivated certain assumptions relative to the visual perceptual ability of an observer. These assumptions, and the definition on which they are based, are fundamental in the problem. Explicitly, the assumptions are:

Assumption (1) The ability of an operator is a function only of C , which characterizes the background illumination of the tube; and of D , which characterizes the relative difference of intensity between the light and dark areas of the tube face.

Assumption (2) This ability is a monotonically increasing function of D for any arbitrary value of C between zero and its saturation value.

III.2.2 Statistical Nature of the Noise Background

Following Rice,¹ we shall consider the noise background to be due to an infinite set of harmonic oscillators of random phase. According to this view, a subset of these oscillators is regarded as operating at a series of equally spaced frequencies, and a passage to a limit is visualized by a process of filling in the regions between the original frequencies with new oscillators. While this packing in of the frequencies is progressing, the amplitudes of the individual oscillators are reduced in such a way that their total power output remains constant. In general, the power delivered by a set of given oscillators whose frequencies lie in an interval df about a specific frequency f_1 is the function $w(f_1)df$. This function is called the power spectrum of the noise. It characterizes the relative amounts of power output from oscillators at various frequencies.

It is possible on the basis of Rice's statistical model of noise, at least in theory, to answer all of the statistical questions which might be asked about the response of the Graphic Indicator to an excitation which consists of a sinusoidal signal in addition to a noise spectrum of specified shape and extent. In particular, it is possible to express in simple form the expected rate of pulse formation which will be caused by crossings of the bias level in any specified portion of the signal cycle. It is just such quantities which are involved in the functions C and D discussed in the previous section.

The assumptions which concern the noise power spectrum are closely related to those which characterize the amplitude spectrum of the filter of the device under consideration. The spectrum that must be used in the Rice theory, which pertains to the statistical properties of the filtered noise, is the product of the filter spectrum and the spectrum of the ambient noise. For convenience in terminology, the point of view is adopted here that the shape of the product spectrum is due to the ambient-noise spectrum alone. The upper and lower ends of the range of frequencies received at the pulse generator are to be considered as corresponding to the upper and lower edges of a rectangular passband of the filter. There is no loss in generality by this division of burden between the noise and the device in characterizing the noise, which is actually presented on the screen.

One basic assumption is made with respect to the noise spectrum.

Assumption (3) The noise is random in the sense just discussed, and the treatment of Rice¹ is applicable.

The report treats two particular power spectra in some detail. Represent the circular frequency of the sinusoidal signal it is desired to detect by f_0 . Denote by θ the fraction of the passband (or noise spectrum) which lies above f_0 , and by a , the total width of this frequency band. In these terms, the cases considered are:

Case I ("white" noise)

$$w(f) = \begin{cases} 0, & f < f_0 - (1 - \theta)a \\ k, & f_0 - (1 - \theta)a \leq f \leq f_0 + \theta a \\ 0, & f_0 + \theta a < f \end{cases}$$

¹S. O. Rice, I. Mathematical Analysis of Random Noise, BSTJ 23: 282-332 (1944)

II. Mathematical Analysis of Random Noise, BSTJ 24: 46-156 (1945)

III. Statistical Properties of a Sine Wave Plus Random Noise, BSTJ 27: 109-157 (1948)

These will be referred to as Rice I, II, III respectively.

function must be known completely if a true optimization is to be performed analytically. Unfortunately, it is not yet known how ability varies with the value of C . Although this precludes a complete optimization, we may arrive at a useful result if we suppose that C is a constant, fixed throughout the analysis, and maximize D .

In analytical terms, then, the optimization which can be undertaken here consists of choosing the design parameters to maximize D , subject to the constraint $C = \text{constant}$. In general, these maxima are not stationary values, and cannot be obtained simply by setting appropriate derivatives equal to zero. One is forced to use a geometrical argument, as described below.

Express the results of Appendix III by the symbolic forms:

$$C = C(\alpha, \beta, \theta), \quad (22)$$

$$D = \tanh(\sigma z), \quad (23)$$

$$z = z(\alpha, \beta, \theta). \quad (24)$$

Denote by $(\alpha_m, \beta_m, \theta_m)$ the triple of values of design parameters which maximizes D , subject to the constraint $C = C^*$, a constant. It is clear from a knowledge of the properties of the hyperbolic tangent function that if the maximization is performed at a fixed value of the signal-to-noise ratio, maximization of D is equivalent to maximization of z .

The most convenient point of view to adopt toward Equations (22) and (24) is geometrical. This keeps in the fore the possibility and significance of nonstationary extrema. Consider θ a parameter, and consider that it is temporarily held constant. Then in a Cartesian three-space of the variables (z, α, β) , Equation (22) represents a cylinder whose generators are parallel to the z -axis. In the same space, Equation (24) represents a general surface. Each of these surfaces carries the parameter label θ . Considering the equations simultaneously is equivalent to considering the curves of intersection of the surfaces. The point on this curve of intersection which it is desired to find is the one whose z -value is greatest. It is also possible to obtain useful results by projecting the curve of intersection into some plane containing the z -axis, and seeking the highest point (i.e., the point with greatest z -value) of this projected curve.

In particular, the curve of intersection may be projected into the $z\alpha$ -plane by eliminating β between Equations (22) and (23). It can be shown, provided only that $w(f)$ is a nonincreasing function of frequency, that at any value of α and for any fixed C^* , the projected curve can only rise as θ is increased. This means that its maximum value must increase as θ increases. Therefore, the maximum point on the intersection of the surfaces is given its largest value when θ is taken as large as possible (namely, $\theta = 1$). It is precisely this condition that one requires in asking that D (or z) be a maximum with respect to θ . It can be concluded that

$$\theta = 1 \quad (25)$$

is an optimum parameter value for any value of C^* . The analytical work accompanying this argument appears in Appendix IV.

Using this result in Equations (22) and (24), one can proceed to find the optimum values of α and β . One possible path of procedure at this point is to consider the intersection of the curve of intersection of surfaces with the radial plane $\phi = \text{constant}$, where

$$\left. \begin{aligned} \alpha &= \rho \cos \phi \\ \beta &= \rho \sin \phi \end{aligned} \right\} \quad (26)$$

The space curve pierces the plane at two points, of which one will generally be higher than the other. The value of ρ , which describes the higher point, is the optimum corresponding to the specific fixed value of ϕ which has been used. As a final step, the radial plane may be rotated to sweep out the angles $0 \leq \phi \leq \pi/2$ (or whatever range of ϕ is physically admissible). The vertical progress of the ρ_m -point can be noted. The value ϕ_m for which this point is a maximum gives the optimum value of the ratio β/α . From ϕ_m and ρ_m , both α_m and β_m can be found. It may be said that ρ_m will generally have to be found by solving a transcendental equation.

These remarks outline the rationale for the general problem of optimizing α and β when $w(f)$ is given. The specific cases of white noise and 6-db noise are treated in some detail in Appendixes V and VI respectively. In these analyses, only the case $C^* > 1$ is treated. It is not implied that the case $C^* < 1$ is of no practical interest, or that it cannot be analyzed within the framework of the present treatment. It is rather that this case will not yield physically meaningful results without introducing further specific assumptions respecting the electronic details of the device. Such an additional program is not within the scope of this report.

The results of the optimization problem may be summarized as follows. If one accepts the model of Section III.2, one can use the optimization process which has been developed to find the optimum design parameters corresponding to any preassigned value of C^* . It is shown in Section III.4.3 that with a particular operational use in mind, an (extensive) experimental program can be made to yield the value of this last unknown parameter. This completely specifies the device which has, subject to the requirements of its intended use, optimum antinnoise characteristics.

III.4 SUMMARY OF RESULTS

III.4.1 Mathematical Results and their Interpretation

For all values of C^* , and all power spectra which are nonincreasing with frequency,

$$\theta_m = 1.$$

Physically, this means that the filter passband should be set so that the operating frequency f_0 lies at its lower edge.*

For the case $C^* \geq 1$, the following results are obtained for the case of white noise in Appendix V.

(a) α_m is the real root of

$$\frac{\alpha(3 + 2\alpha)}{3 + 3\alpha + \alpha^2} = \ln \left[\frac{3 + 3\alpha + \alpha^2}{3C^{*2}} \right] \quad (27)$$

*It is recognized that physical considerations may prevent making θ quite as large as 1. The value that would give best results, then, is the largest value compatible with these physical considerations.

(b) z_m is found from α_m by

$$z_m = \left[\frac{(3 + 2\alpha_m)}{3 + 3\alpha_m + \alpha_m^2} \right]^{1/2} \quad (28)$$

(c) β_m is found from α_m and z_m by

$$\beta_m = \alpha_m z_m \quad (29)$$

The physical interpretation of these results are:

- (a) That there is a unique optimum bandwidth, which increases with increasing C^* , and
- (b) That there is a unique optimum bias, which increases with increasing C^* .

Again for the $C^* \geq 1$, the case of 6-db noise treated in Appendix VI, gives the results:

- (a) $\alpha_m = \alpha^*$, where α^* is the largest bandwidth which can be used in view of any other operating considerations,

$$(b) \quad \beta_m = \left[\left(\frac{1 + \alpha^*}{\alpha^*} \right) \ln \left(\frac{1 + \alpha^*}{C^{*2}} \right) \right]^{1/2}, \text{ and} \quad (30)$$

$$(c) \quad z_m = \left(\frac{1 + \alpha^*}{\alpha^*} \right) \beta_m. \quad (31)$$

If α^* is known, both β_m and z_m are easily obtained from Equations (30) and (31). It is unnecessary in this case to solve a transcendental equation. The physical interpretation of the results for this special case is:

- (a) That there is a unique optimum bandwidth, which is equal to the largest bandwidth that can be realized practically, and
- (b) That there is a unique optimum bias, which approaches zero as α^* is increased indefinitely.

Results for the case $C^* < 1$ cannot be made as complete as those above without a somewhat more detailed model for the device. However, some general statements as to the nature of the mathematical optima can be given.

Regardless of the form of $w(f)$, Equation (60) shows that z (and therefore D) can be made greater than any preassigned positive number by the choice of a sufficiently small bandwidth. This is true because as $a \rightarrow 0$, $\psi \rightarrow 0$ and $\psi''/\psi \rightarrow \text{constant} \neq 0$, while the condition $C^* < 1$ insures that a solution of this equation for z shall always exist. Although the behavior of D with bandwidth at larger bandwidth is dependent upon the specific form of $w(f)$, Table III.1 will illustrate the general nature of this behavior, using power spectra of the form $w(f) = 1/f^n$. Thus, there are at least some noise spectra for which D approaches large (possibly infinite) values for sufficiently large bandwidths.

TABLE III.1
Behavior of D at Large Bandwidth for $w(f) = 1/f^n$

n	$\lim_{a \rightarrow \infty} D$
0 (white noise)	$\rightarrow 0$ asymptotically from above
1 (3-db noise)	\rightarrow constant > 0 asymptotically from below
2 (6-db noise)	$\rightarrow \infty$
3 (9-db noise)	$\rightarrow \infty$
> 3	\rightarrow constant > 0 asymptotically from below

These results may be interpreted as follows. Since some power is required to actuate the p/p generator, the infinite value of D at vanishingly small bandwidth is not physically realizable. It is equally evident that one cannot in practice extend the passband to infinity. In both cases, the maximum practicable value of D is set by the specific electronic design of the apparatus. It is therefore impossible to state a priori which of the two cases is the over-all practicable optimum. One cannot even preclude the possibility that relative (stationary) maxima of D exist for $0 < a < \infty$, and that such stationary maxima might exceed the greater practicable value of D obtainable at the extremes of bandwidth.

Summarizing, one sees that for the case $C^* < 1$ the analysis is strongly influenced by the specific electronic design of the apparatus, and less strongly by the specific form of $w(f)$. It is to be understood, however, that the optimization problem for $C^* < 1$ is completely tractable by the methods of this report when a spectrum $w(f)$ and a sufficient set of conditions on the electronic details of the device are specified.

III.4.2 Results of Immediate Applicability

The result $\theta_m = 1$ is true for any power spectrum $w(f)$ which is nonincreasing with frequency. Because the result is so general, one can conclude at once that the device should be designed so that its passband lies entirely above the operating frequency, insofar as this can be done. A case in which it cannot be done is one in which the location of the working frequency is imperfectly known a priori, or is subject to variation during the course of an observation. In such a case, the passband should be chosen to lie entirely above the lowest anticipated working frequency.

The nature of the optimum bandwidth depends markedly upon the power spectrum of the background noise. It is therefore clear that the nature of the noise background in which it is expected to work must be determined experimentally, to provide more realistic design information. A corollary of this observation is that any noise source to be used with profit in the laboratory must have a spectrum closely approximating the noise to be found under conditions of actual use.

III.4.3 Extension of the Results

The impossibility of completing an over-all optimization on the basis of the model of the Graphic Indicator developed in Section III.2 has been discussed in Section III.3. There, the optimization is carried as far as permitted by theoretical considerations alone. It remains to see what further information is required to characterize completely the ability of an operator to detect a given signal with the optimum device, and to answer the question of what threshold signal can be detected with it.

Although it was postulated that "ability" was a function of C and D only, no objective definition of ability has yet been given. For the purposes of this discussion, the value of the ability function is to be understood as being identical with the probability that a random observer give a correct answer to the question "Is there a signal present?" This definition gives the ability function (which will be denoted by Q) the properties that are required by more subjective points of view.

In symbolic terms, it has been assumed that

$$Q = Q[C^*, D(\sigma, z)]$$

where Q is monotone increasing with D at constant C^* . It has been deduced that D is monotone increasing with σ , the signal-to-noise ratio, at constant z . For an optimum device at C^* , i.e., one whose parameters have been optimized while holding $C = C^*$, one finds a result:

$$z_m = z_m(C^*),$$

which reduces Q to the form

$$Q = Q_m(C^*, \sigma).$$

By the previous remarks, the function Q_m has the property of being monotonically increasing with σ at constant C^* . However, since no assumption has been introduced about the behavior of Q with C^* , no deduction is possible respecting the behavior of Q_m with C^* at constant σ . It is this behavior which must be obtained experimentally.

One may proceed as follows. Select a particular value of C^* , say C_1^* , and adjust the device to be optimum at C_1^* . Expose a number of observers to the presence of signals corresponding to a range of signal-to-noise ratios, and calculate the ability function by the probability definition given previously. This provides a relationship $Q = Q_m(C_1^*, \sigma)$ whose plot in the Q, σ plane will be (qualitatively) as indicated in Figure 15. Select another value C_2^* , readjust the physical parameters of the device accordingly, and determine $Q = Q_m(C_2^*, \sigma)$ by the same procedure. A continuation of the process generates a family of curves in the Q, σ plane. Each member of the family corresponds to a particular value of C^* , and therefore to a particular set of physical parameters.

The value of C^* which is chosen as optimum by the designer depends upon the manner in which the members of this family of curves intersect one another. There are two mutually exclusive possibilities:

- (a) There is a unique curve $Q = Q_m(C_m^*, \sigma)$ which lies entirely above every other member of the family. In this case, the design parameters corresponding to C_m^* give an absolutely optimum device. It will be fortunate

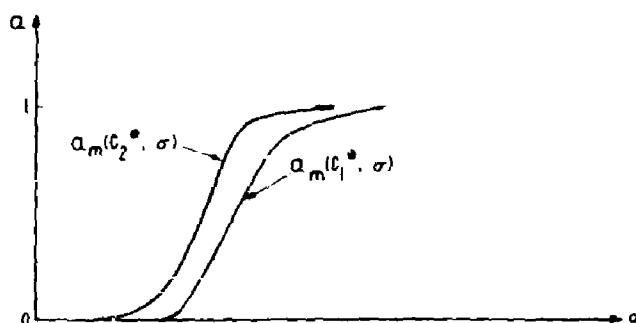


Figure 15 - Dependence of a_m upon C^* and σ

if this case exists in practice, for then the optimum device is independent of the signal-to-noise ratio which may maintain at any time.

(b) The curves of the family cross one another in such a way that there are only limited ranges of σ within which a single curve lies above all other members of the family. For adjacent ranges of σ , this curve will generally be replaced by some others as highest curves. The value of C^* to be employed in practice must be dictated by the operational requirements of the device (e.g., the requirement that only abilities above a certain value are acceptable, no matter what value of σ maintains). It is fruitless to speculate further at this time as to the possible operational requirements which could completely determine the optimum C^* in this case.

APPENDIX I

Basic Patterns Produced by a Superposition of Two Sinusoids

It is the primary purpose of the present Appendix to derive the qualitative appearance of the presentation when the input consists of a superposition of two sinusoids. A secondary purpose is to provide a framework for such exact quantitative treatment as might, in the future, be required. Our attention will be principally focused upon the dependence of the presented pattern upon the amplitude ratio of the constituent sinusoids.

Let us, at the outset, discuss the gross features of such a presentation. Taking the input to be the superposition of two sinusoids

$$\xi_1 = A_1 \sin(\omega_1 t - \phi) \quad (32)$$

$$\xi_2 = A_2 \sin(\omega_2 t - \phi)$$

where an appropriate shift in the origin of time has made the phase angles equal, we adopt the convention that ω_1 shall always refer to the higher frequency, so that the frequency ratio, r , shall be given by

$$r \equiv \frac{\omega_2}{\omega_1} < 1 \quad (33)$$

The first gross feature results from the phenomenon of beats. To display the beats, it is convenient to manipulate $\xi = \xi_1 + \xi_2$ into the form

$$\begin{aligned} \xi = \xi_1 + \xi_2 = & \left[A_1^2 + A_2^2 + 2A_1 A_2 \cos \left\{ (\omega_1 - \omega_2)t \right\} \right]^{1/2} \sin \left[\frac{(\omega_1 + \omega_2)}{2} t \right. \\ & \left. - \phi + \tan^{-1} \left\{ \frac{A_1 - A_2}{A_1 + A_2} \tan \frac{(\omega_1 - \omega_2)t}{2} \right\} \right] \end{aligned} \quad (34)$$

which will be recognized as a sinusoid having a time-dependent phase angle and a time-dependent amplitude.

In the case of the Graphic Indicator, we are always interested in those cases for which ω_1 is nearly equal to ω_2 , i.e., where

$$(1 - r) \ll 1 \quad (35)$$

Roughly speaking, the sinusoid is hence of frequency ω_1 (or ω_2), and the amplitude is periodic with period $2\pi/\omega_1 - \omega_2$. The subsequent analysis will confirm what we might at once suspect: that the precise locations of the spots on the presentation are determined almost entirely by the maxima of the sinusoid, and the gross form of the presentation is determined almost entirely by the time-dependence of the amplitude, and that, in particular, the presentation is very nearly periodic with period $2\pi/\omega_1 - \omega_2$. This is the first gross feature to be noted.

Secondly, one should note that the amplitude becomes a minimum at instants

$$t = \frac{1}{\omega_1} \frac{(2N + 1) \pi}{1 - r}; N = 0, 1, 2, 3, \dots \quad (36)$$

Immediately prior to and subsequent to these instants the automatic gain control will prevent the formation of spots irrespective of the maxima of the sinusoidal factor of Equation (34), so that the times of occurrence of such spots are of merely mathematical (rather than physical) interest.

A third gross feature to be noted is that, because of Equation (35), there are many maxima of the sinusoid (and hence many spots) in each period of duration $2\pi/\omega_1 - \omega_2$, and hence many spots in each period of the presentation. Physically, we are therefore allowed to ignore any small number (of the order of 1 or 2) of spots per period $2\pi/\omega_1 - \omega_2$, inasmuch as it is evident that the arbitrary displacement of such a small number of spots is incapable of altering the shape of the presentation.

These facts allow us to exclude from consideration certain special cases whose complete analysis has been shown to be mathematically complex but physically trivial, and to give a purely graphical solution to our problem.

It is convenient to return to Equation (32), and assume* that a spot is produced at instants $t_s = \tau_s/\omega_1$, if and only if

$$\left(\frac{d\xi}{dt} \right)_{t=t_s} = 0 \quad (37a)$$

and

$$\left(\frac{d^2\xi}{dt^2} \right)_{t=t_s} < 0 \quad (37b)$$

Subject to the restrictions stated, Equation (37a) is equivalent to

$$\tan(\tau_s - \phi) = - \frac{1 + \lambda \cos(1 - r)\tau_s}{\lambda \sin(1 - r)\tau_s} \quad (38a)$$

where

$$\tau_s = \omega_1 t_s \quad (38b)$$

and

$$\lambda = \frac{A_2 \omega_2}{A_1 \omega_1}, 0 < \lambda < \infty \quad (38c)$$

*Whether one assumes that a spot is produced when Equation (37) is satisfied, or whether (as in Part III) when the excitation exceeds a fixed bias level, would seem physically inconsequential. The criterion used here is more tractable for continuous and completely determined functions of the type we are now considering, while the second criterion is mathematically more suitable when the function is given statistically.

Restrictions are that

$$(1 - r)\tau_s \neq N\pi, N = 0, 1, 2, 3, \dots \quad (38d)$$

and

$$(\tau_s - \phi) \neq (2M + 1)\frac{\pi}{2}, M = 0, 1, 2, \dots \quad (38e)$$

where, as may be shown, (38d) implies (38e) and vice versa.

Equation (38a) gives the maxima and minima of ξ , and in addition the inflection points of ξ . It may be shown that all possible inflection points of ξ lie in intervals of τ_s , $\left(\frac{(2M + 1)\pi}{1 - r} - \pi, \frac{(2M + 1)\pi}{1 - r} + \pi\right)$, $M = 0, 1, 2, 3, \dots$, i.e., as may be seen from Equation (36), in the intervals just preceeding and following the minima of the amplitude factor of Equation (34). Because of the AGC action, the spots (at most three) which might appear in each such interval will actually be missing from the presentation. Provided (as we shall) that we exclude from further consideration any solutions of Equation (38) which appear in such intervals, the continuity of ξ and its derivatives assures that alternate solutions of Equation (34) are maxima (and hence spots), and that the intervening solutions are minima (and hence not spots).

Deferring* until later the determination of which solutions of Equation (38a) are spots (and which are not spots), it is evident that the solutions themselves may be obtained by the intersections of graphs of the left- and right-hand members. The left-hand member (denoted by LHM) is a function of the variable τ_s and of the parameter ϕ . The qualitative appearance of the Graphic Indicator presentation is independent of the value of the latter, and no importance should be attributed to the arbitrary selection of the value of ϕ used in Figure 16,[†] to which the reader is referred.

The right-hand member (RHM) is independent of ϕ , and is a function of the variable τ_s and of the parameters r and λ . For any fixed ω_1 and ω_2 (the former, we recall, being always the higher circular frequency), the specification of λ is equivalent to the specification of the amplitude ratio, A_1/A_2 . The appearance of the presentation for all possible values of the amplitude ratio may accordingly be derived by allowing λ to pass through its complete range $(0, \infty)$.

The dependence of RHM upon λ may be best explained by the consideration of 3 natural cases, the first and last of which we may further subdivide into 2 sub-cases:

$$\left. \begin{array}{l} \lambda < 1 \left\{ \begin{array}{l} \lambda \ll 1, \text{ (A)} \\ \lambda \approx 1, \text{ (B)} \end{array} \right\} \\ \lambda = 1 \\ \lambda > 1 \left\{ \begin{array}{l} \lambda \approx 1, \text{ (A)} \\ \lambda \gg 1, \text{ (B)} \end{array} \right\} \end{array} \right\} \quad \begin{array}{l} \text{I} \\ \text{II} \\ \text{III} \end{array} \quad (39)$$

*It may be shown analytically that irrespective of the value of λ , that if ϕ is contained in the first and fourth quadrants that the first, third, fifth, etc., solutions of Equation (38) are spots; while if ϕ is contained in the second or third quadrants, that the second, fourth, sixth, etc., solutions are spots. This counting process is, however, cumbersome as compared to a graphical procedure which will shortly be presented.

[†]Figure 16 appears on page 65.

Sketches of RHM for five such values of λ are shown in Figure 17. Although these are typical, the following general analytical information about RHM may be stated.

In all cases listed, RHM is periodic with period $2\pi/1 - r$.

Case I, $\lambda < 1$

$$\text{RHM} < 0, \frac{2N\pi}{1-r} < \tau_s < \frac{(2N+1)\pi}{1-r}; N = 0, 1, 2, 3, \dots$$

$$\text{RHM} > 0, \frac{(2N+1)\pi}{1-r} < \tau_s < \frac{(2N+2)\pi}{1-r}; N = 0, 1, 2, 3, \dots$$

Zeros - none

Singularities - at $N\pi/(1-r)$, $N = 0, 1, 2, \dots$, as sketched in Figures 17a, 17b.

Within any half-period, i.e., within any range such that

$$\frac{N\pi}{1-r} < \tau_s < \frac{(N+1)\pi}{1-r}, N = 0, 1, 2, 3, \dots$$

RHM possesses a stationary (maximum or minimum) value of magnitude

$$\left| \frac{\sqrt{1-\lambda^2}}{\lambda} \right|$$

which occurs at the point $\tau_s^{(s)}$ given by

$$\tau_s^{(s)} = \frac{\arccos(-\lambda)}{1-r}$$

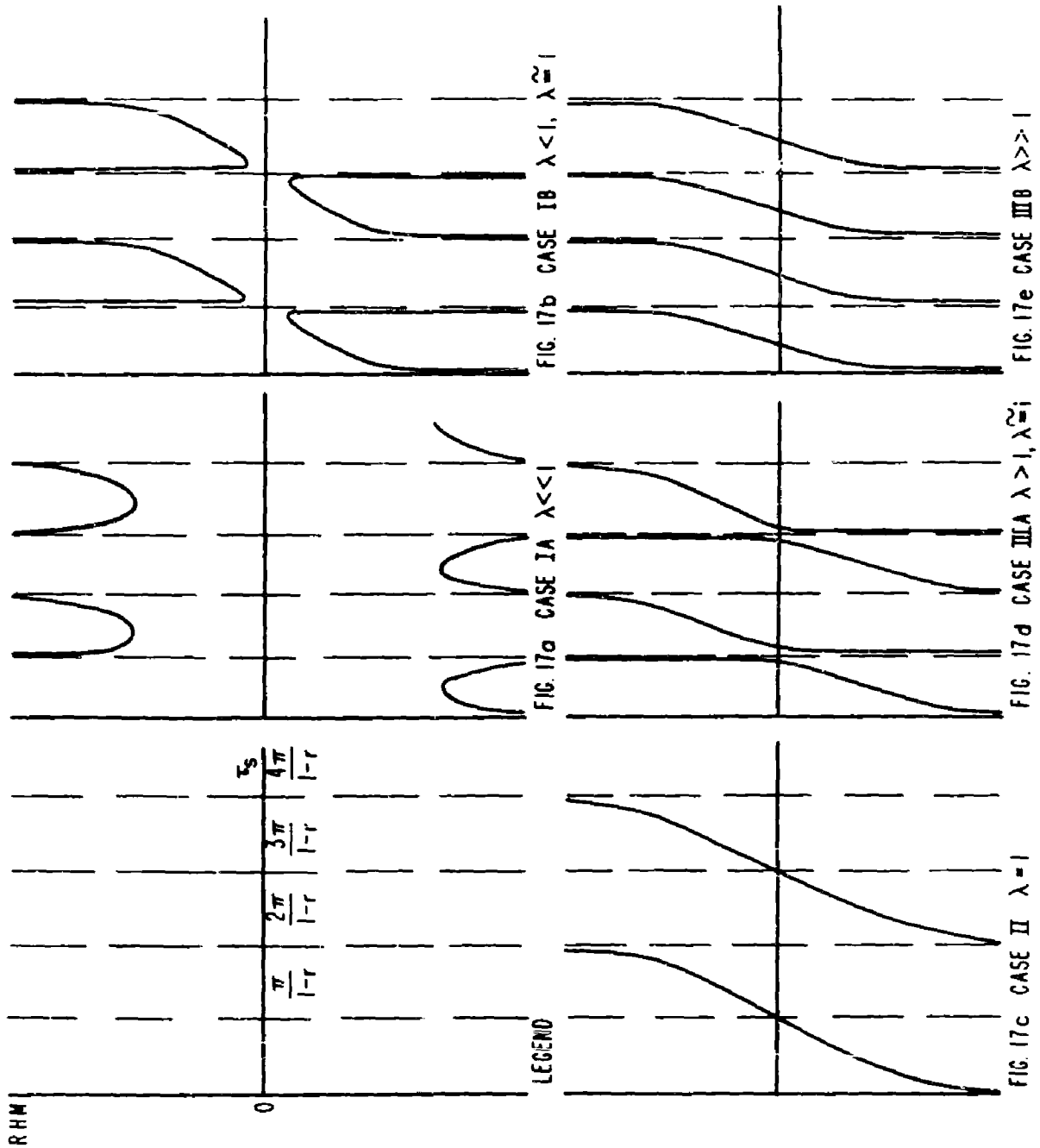
Subcase IA, $\lambda \ll 1$

For $\lambda \ll 1$, the magnitude of the stationary value is approximately $\left| \frac{1}{\lambda} \right|$, and RHM consequently remains far from the axis of τ_s . In each half period, the function RHM is approximately symmetric about the midpoint of the half period, since

$$\tau_s^{(s)} \cong \frac{\arccos(-0)}{1-r} = \frac{(2N+1)\pi}{2(1-r)}, N = 0, 1, 2, \dots$$

Subcase IB, $\lambda \cong 1$

For $\lambda \cong 1$, the magnitude of the stationary value is almost zero, and RHM consequently almost intersects the axis of τ . However, RHM is



decidedly antisymmetric about the midpoint of each half period, since

$$\tau_s^{(a)} \cong \frac{\arccos(-1)}{1-r} = \frac{(2N+1)\pi}{1-r}, N = 0, 1, 2, 3, \dots,$$

the stationary values occurring close to the odd multiples of $\pi/(1-r)$.

Case II, $\lambda = 1$

RHM $\cong -\cot \frac{(1-r)\tau_s}{2}$, a well-known function which is adequately sketched in Figure 17c.

Case III, $\lambda > 1$

Zeros - At $\cos(1-r)\tau_s = -1/\lambda$.

In any complete period, $\frac{2N\pi}{1-r} < \tau_s < \frac{(2N+2)\pi}{1-r}$, $N = 0, 1, 2, \dots$, there are consequently two zeros, $\tau_s^{(0)}$, the first in the interval

$$\frac{(2N+1/2)\pi}{1-r} < \tau_s^{(0)} < \frac{(2N+1)\pi}{1-r},$$

and the second in the interval

$$\frac{(2N+1)\pi}{1-r} < \tau_s^{(0)} < \frac{(2N+3/2)\pi}{1-r}$$

the exact locations of these zeros depending upon λ .

Singularities - At $\tau_s = N\pi/(1-r)$, $N = 0, 1, 2, \dots$, as sketched in Figures 17d and 17e.

Subcase III A, $\lambda \cong 1$

In each period, $\frac{2N\pi}{1-r} < \tau_s < \frac{(2N+2)\pi}{1-r}$, $N = 0, 1, 2, \dots$, the zeros immediately precede and follow $\tau_s = \frac{(2N+1)\pi}{1-r}$.

Subcase III B, $\lambda \gg 1$

In each period, $\frac{2N\pi}{1-r} < \tau_s < \frac{(2N+2)\pi}{1-r}$, $N = 0, 1, 2, \dots$, the first zero immediately follows $\tau_s = \frac{(2N+1/2)\pi}{1-r}$, and the second immediately precedes $\tau_s = \frac{(2N+3/2)\pi}{1-r}$.

With this information about the influence of λ upon the form of RHM we may proceed to the graphical solution of Equation (38a). In Figures 18 to 22† are presented the superposition of Figure 16 (LHM) upon the curves of Figure 17 (RHM). The intersections of LHM with RHM represent all of the solutions of Equation (38a), both maxima and minima.

It remains merely to decide which solutions are which, a question easily settled. From the form of Equation (32) it is apparent that for fixed ω_1 and ω_2 the dimensionless times, τ_s , corresponding to the maxima of ξ are continuous in A_1 and A_2 . The same statement may be made for the minima of ξ . For fixed r , the dimensionless times, τ_s , corresponding to maxima are accordingly continuous in λ . Any particular branch of LHM accordingly possesses a maximum of ξ (and hence a spot) for all values of λ , if it possesses a maximum for any value of λ . The same statement applies to the minima. Inasmuch as allowing λ to approach 0 is equivalent to allowing A_2 to approach 0, the maxima of ξ in this limiting case must occur at instants which approach certain of the asymptotes of LHM, namely those at

$$\tau_s = \phi + (4N + 1)(\pi/2), N = 0, 1, 2, \dots \quad (40)$$

and the branches of LHM which possess maxima may be accordingly found by noting which solutions occur closest to these values in Subcase I A ($\lambda \ll 1$). For purposes of convenience, the asymptotes of LHM given by Equation (40) have been drawn heavy in Figures 18 to 22.

Having determined the times of occurrence of the spots, it remains to relate these times to the appearance of the presentation.* To do so, it is easiest first to discuss the presentation for the case when the reference frequency is made equal to ω_1 (the higher frequency), and to obtain from this case the presentations for other values of the reference frequency.

In Figures 18 to 22 are drawn arrows† to indicate the time intervals by which the spots which are produced by ξ lead or lag the spots which would be produced if ω_1 alone were present in the input (i.e., if λ were zero). If leads are plotted negatively and lags positively, the resulting plot will be in correspondence with the appearance of the presentation when the reference frequency is made equal to ω_1 ; this has been done in Figure 23 for the values of λ corresponding to Cases IA, IB, II, IIIA, and IIIB.** The dotted portions of the curves indicate the regions where the AGC action actually suppresses the formation of spots.

*For purposes of describing the presentations which one observes on the Graphic Indicator, it is unnecessary to give more than a qualitative discussion of the times of occurrence of the spots. For specific values of the parameters λ , ϕ , and r , the discussion may, of course, be made as quantitative as one desires; in particular, the time of occurrence of any spot may be determined numerically with arbitrarily small error. Because of the nature of the problem, it is however impossible to express the spot-times as a finite sum of elementary functions of the parameters.

**Inasmuch as the precise locations of individual spots are unimportant in determining the shape of the observed pattern, it is sufficient in Figure 23 (and in similar sketches to follow) to fair a line through the spots. Furthermore, because of the actual overlapping of the cathode-ray spots in practice, it is more realistic to portray a line. As is implied in the text, the more obvious qualitative features of these lines may be inferred from the time intervals which are indicated in Figures 18 to 22. This is true, in particular, for the signs of the slopes and for the vertical extents of the lines. However, the signs of the curvatures can be inferred in this way only for small λ ; and the curvatures for large λ have been determined from other considerations.

†Figure 18 appears on page 65; Figures 19 and 20 on page 67; and Figures 20 and 21 on page 69

‡Marked with stars, viz: ★

The patterns are obviously periodic.* Furthermore, the reader will note that the magnitude of the maximum spot-time discrepancy which occurs in each half period (of length $\pi/(1-r)$) increases with increasing λ ; and that the sense of the discrepancy reverses at the odd multiples of $\pi/(1-r)$, the magnitude of the reversal also increasing with increasing λ . The existence of these periodic sudden reversals in the sense of the spot-time discrepancy is important in providing a means of recognizing and identifying the patterns.

The patterns of Figure 23 are not unique, since their appearance may be materially altered by arbitrary changes in the phase (say ψ) of ω_1 , the higher constituent frequency, with respect to the phase of the reference frequency. Equivalently, one may regard any plane presentation as having been obtained from a more fundamental presentation plotted upon the surface of a right circular cylinder. From this viewpoint, the cutting of the cylinder along any generator is equivalent to the selection of some particular value of ψ , the cut edges becoming the top and bottom of the plane figure obtained by unrolling the cylindrical surface. For example, if ψ is shifted by π , the presentations of Figure 23 appear as in Figure 24. In the latter, the patterns are characterized by horizontal rows of holes which are associated with the previously mentioned reversals in the sense of the spot-time discrepancy.

The foregoing remarks about the lack of uniqueness of the plane patterns displayed on the Graphic Indicator are perfectly general, and are valid for all values of the reference frequency. In our subsequent discussion of the patterns obtained when the reference frequency is unequal to ω_1 , we shall display those patterns which seem most important. It should, however, be understood that from each pattern which we shall display may be made an infinity of correct and experimentally realizable patterns. This may be done by rejoining the top and bottom of our pattern and recutting the resulting cylinder along any arbitrary generator.

Inasmuch as the spatial discrepancy between the line of spots produced by two sinusoids and the line which would be produced if ω_1 alone were present is nearly independent of the value of the reference frequency,** the patterns for any other value of the reference frequency may be inferred from the patterns of Figure 23. The following construction in Figure 25 will illustrate the method.

Of particular interest in practice are the patterns which are periodic in space, or which would be if the horizontal sweep were sufficiently slow. One may in general achieve periodicity in two ways, (a) by a suitable adjustment of the reference frequency with respect to the values of ω_1 and ω_2 (periodicity of this type is independent of the value of r , and in particular of whether or not ω_1 and ω_2 are commensurate) or (b), by choosing ω_1 and ω_2 to be commensurate. The discussion of (a) alone is germane to the applications of the Graphic Indicator which are at present contemplated.

*That is, they are periodic for all practical purposes. The error made in replacing the spots by a faired line of constant length per period, $(1/\omega_1)(2\pi/1-r)$, is equivalent to ignoring the errors caused by the addition or deletion of (at most) two spots per period. Thus, although the patterns of Figure 23 are aperiodic in the fine (since the locations of the spots are in general aperiodic), they are periodic in the gross; and it is only the gross appearance which is subject to observation and experiment.

**The temporal discrepancies between these sets of spots are strictly independent of the reference frequency. In practice, the reference frequency, ω_1 , and ω_2 are all almost identical, with the consequence that the spatial discrepancies are similarly independent to within an approximation sufficient for our present purpose.

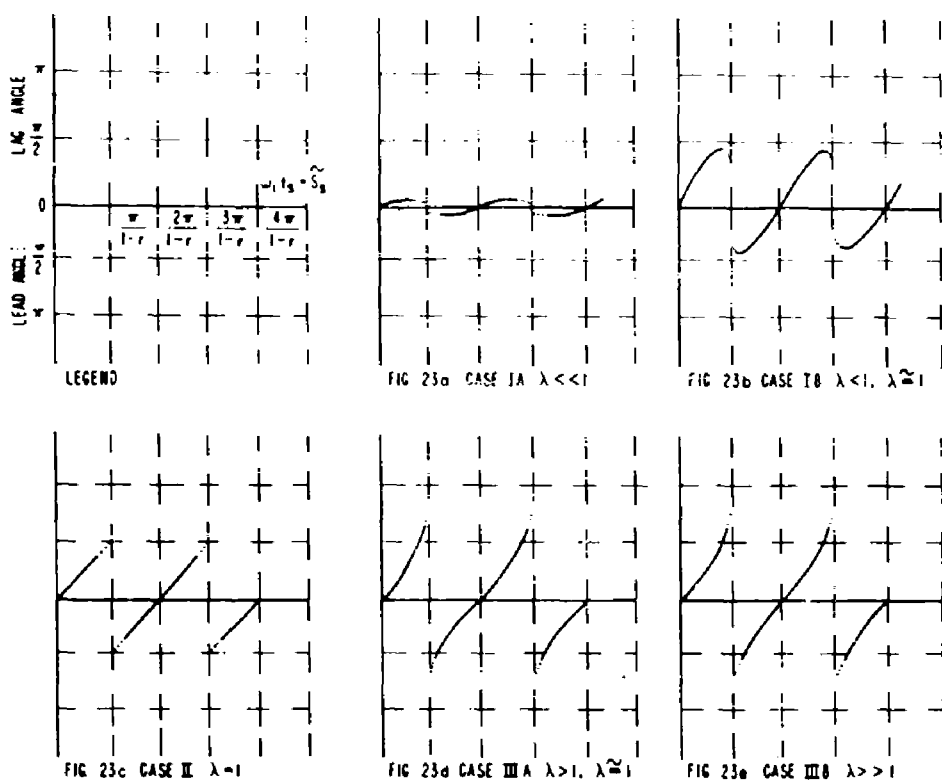
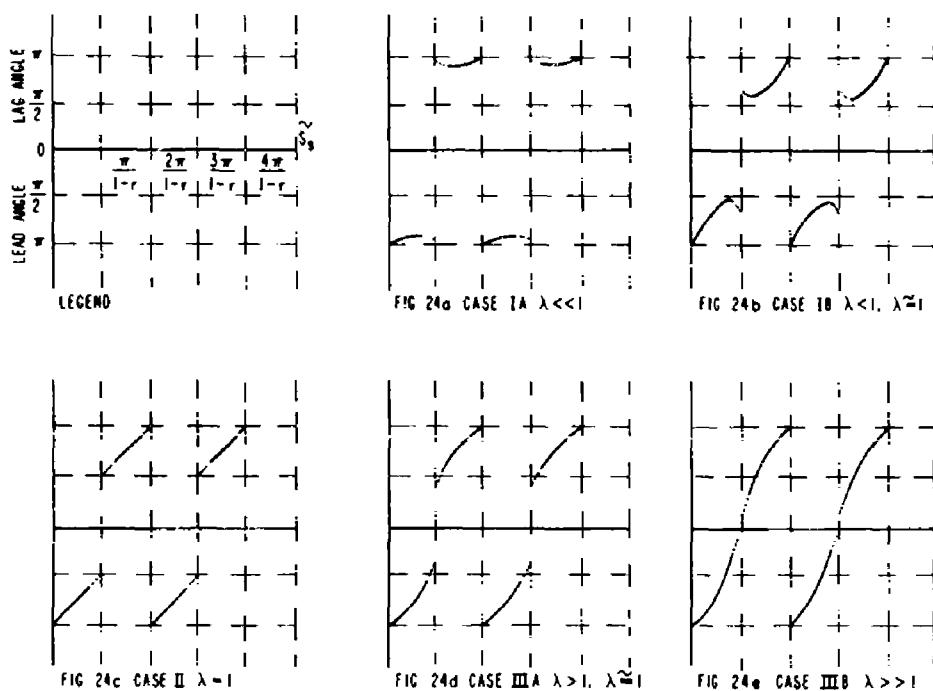

 Figure 23 - Lead and lag angles vs. τ_s


Figure 24 - Change in the patterns of Figure 23 due to a shift in the phase of the reference oscillator

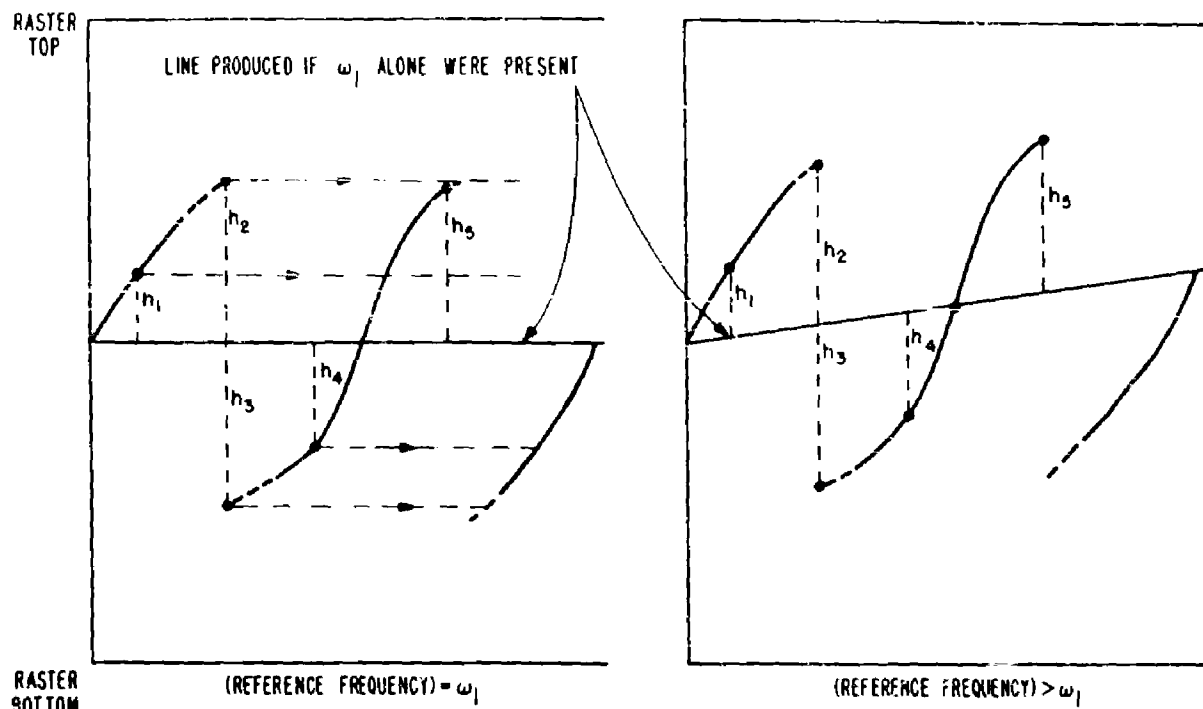


Figure 25 - Change in pattern due to small change in reference frequency

From the previous general discussion of patterns, it will be evident that the presentation will be spatially periodic if the fundamental period of the presentation, $2\pi/\omega_1(1-r)$, is commensurate with the time required for the line of spots caused by ω_1 acting alone to cross the raster from bottom to top (or top to bottom). Using the expression for the slope of a single sinusoid developed in Part I, we find this latter time to be

$$t_c = \mp \left(\frac{2\pi}{\omega_v} \right) \cdot \left(\frac{1}{\omega_1} \right) \quad (41)$$

where ω_v is the vertical or reference frequency, and where the upper sign is to be used if $\omega_1 < \omega_v$ (the line of spots passing from bottom to top), and where the lower sign is to be used if $\omega_1 > \omega_v$ (the line of spots passing from top to bottom). The condition for periodicity in the pattern is hence that

$$pt_c = q \frac{2\pi}{1-r} \cdot \frac{1}{\omega_1}$$

where p and q are positive integers. Expressing ω_v in the form

$$\omega_v = P\omega_1 + Q\omega_2$$

where P and Q are as yet undetermined, these equations yield

$$(1 - P \pm s) + r(-Q \mp s) = 0 \quad (42)$$

where $s = p/q$. Restricting attention to the values of P and Q which satisfy Equation (42) for arbitrary r, we conclude that

$$Q = \mp s \quad (43)$$

$$P + Q = 1$$

For the case $q = 1$ (which necessitates that the pattern be periodic with period $\frac{2\pi}{1-r} \cdot \frac{1}{\omega_1}$) one may develop from Equation (43) the following information.

$s = p$	$t_c = \frac{1}{s} \cdot \frac{2\pi}{1-r} \cdot \frac{1}{\omega_1}$	Slope of ω_1 line	$\omega_v = P\omega_1 + Q\omega_2$
1	$\frac{2\pi}{1-r} \cdot \frac{1}{\omega_1}$	+ -	$2\omega_1 - \omega_2$ ω_2
2	$\frac{\pi}{1-r} \cdot \frac{1}{\omega_1}$	+ -	$3\omega_1 - 2\omega_2$ $-\omega_1 + 2\omega_2$
3	$\frac{2\pi}{3(1-r)} \cdot \frac{1}{\omega_1}$	+ -	$4\omega_1 - 3\omega_2$ $-2\omega_1 + 3\omega_2$
etc.			

Conversely, for the case $p = 1$ (which necessitates that the pattern be periodic with period $\frac{2\pi}{1 - \frac{\omega_v}{\omega_1}} \cdot \frac{1}{\omega_1}$) one may develop

$s = \frac{1}{q}$	$t_c = \frac{1}{s} \cdot \frac{2\pi}{1-r} \cdot \frac{1}{\omega_1}$	Slope of ω_1 line	$\omega_v = P\omega_1 + Q\omega_2$
$\frac{1}{2}$	$\frac{4\pi}{1-r} \cdot \frac{1}{\omega_1}$	+ -	$(3/2)\omega_1 - (1/2)\omega_2$ $(\omega_1 + \omega_2)/2$
$\frac{1}{3}$	$\frac{6\pi}{1-r} \cdot \frac{1}{\omega_1}$	+ -	$4\omega_1/3 - \omega_2/3$ $2\omega_1/3 + \omega_2/3$
etc.			

In addition to the periodic patterns whose descriptions fall within the two cases just considered, there are the patterns for which $p > 1$, $q > 1$. In particular, there are an infinity of periodic patterns for which $\omega_1 > \omega_v > \omega_2$, i.e., those for which $\omega_v = \frac{L\omega_1 + M\omega_2}{L + M}$

where L and M are positive integers. Because of the length of their periods, however, these latter patterns will be observed as periodic only if the horizontal sweep is slow.

For the antireverberation applications of the Graphic Indicator, the periodic patterns for which $\omega_1 \geq \omega_v \geq \omega_2$ are of especial importance. We have already sketched typical patterns for the case $\omega_v = \omega_1$ (Figures 23 and 24). Of the intermediate cases, we shall consider only that for which $\omega_v = (\omega_1 + \omega_2)/2$, a pattern sketched in Figure 26 for the λ cases which we have considered previously. It is to be noted that the patterns for the extreme λ cases ($\lambda \ll 1$, and $\lambda \gg 1$) are each characterized by two rows of horizontal holes, the height of these holes being accentuated by the AGC action.

Finally, we consider the patterns for which $\omega_v = \omega_2$ (the second case of the table for which $q = 1$). These are sketched in Figures 27 and 28 (which is Figure 27 with the phase, ψ , shifted by π) for the λ cases which we have considered previously. Especially noteworthy are the similarities and differences between these and the patterns obtained when $\omega_v = \omega_1$ (Figures 23 and 24). First off, we note what we might have suspected for the extreme λ cases: that in Figures 23 and 24, where $\omega_v = \omega_1$, that the lines of spots tend to be horizontal for low λ (i.e., for $A_1 \gg A_2$); while in Figures 27 and 28, where $\omega_v = \omega_2$, nearly horizontal spot-lines appear for high λ (i.e., for $A_2 \gg A_1$). The detailed behavior with λ of the patterns in Figures 23, 24, 27, and 28 is best appreciated by study of the patterns themselves.

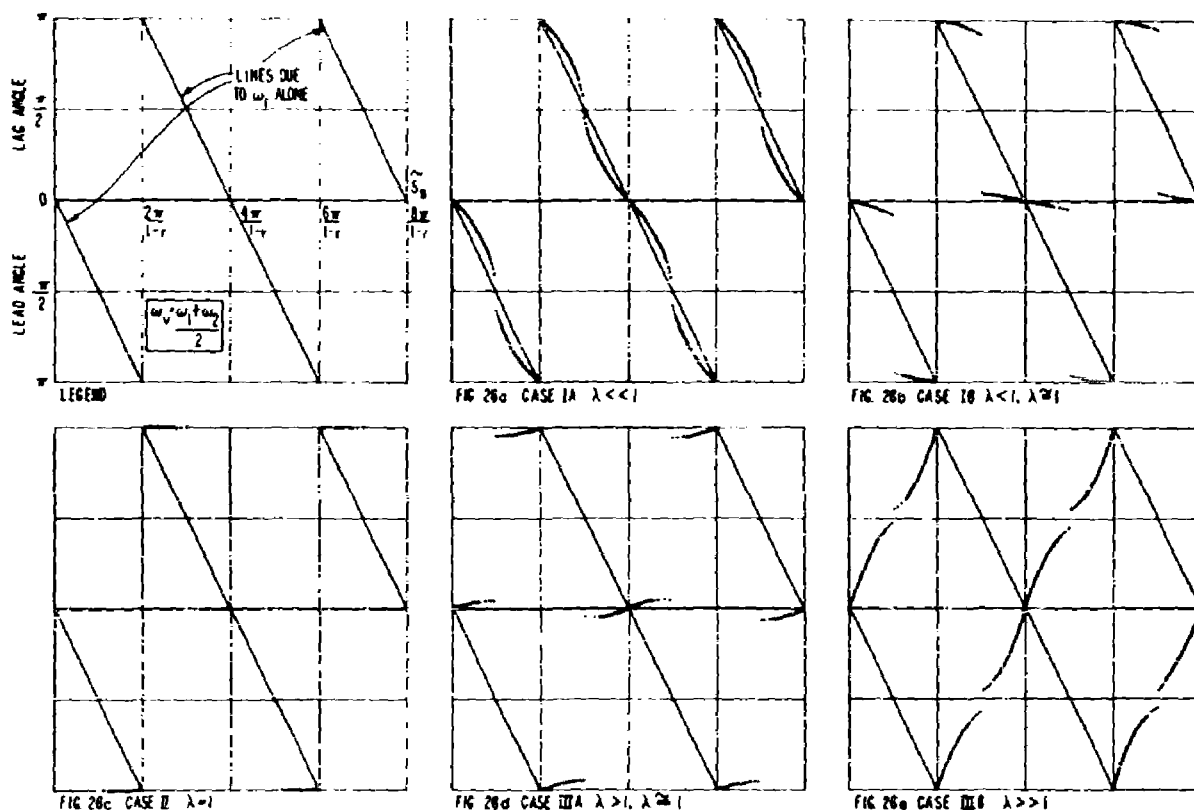


Figure 26 - Presentation when the reference frequency equals the mean of the constituent frequencies

Apart from the behavior with λ , there is, however, one qualitative attribute which makes possible an unambiguous classification of these patterns. This attribute is the "trend of the slope" - i.e., whether the spot-lines tend to be of positive or negative slope. The patterns for $\omega_v = \omega_1$, and $\omega_v = \omega_2$, may be classified on this basis as follows.

ω_v	Trend of the Slope
$\omega_v = \omega_1$	Positive
$\omega_v = \omega_2$	Negative

Alternatively, if one knows that the pattern being viewed is due to two sinusoids, and that one of them is equal to ω_v , he can draw an unambiguous conclusion about which (the higher or the lower) equals ω_v . In the sonar applications of the Graphic Indicator, this attribute enables the operator to determine whether the frequency of a weak echo is higher or lower than that of the background reverberations.

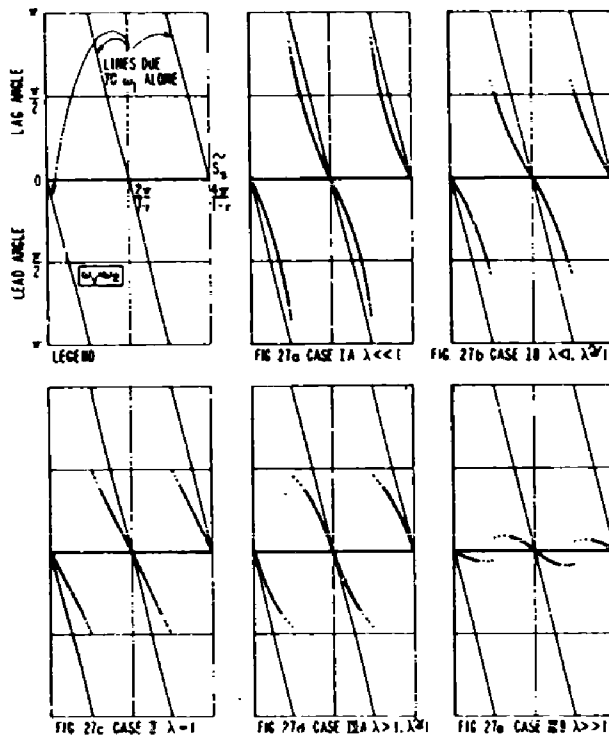


Figure 27 - Presentation when the reference frequency equals the lower constituent frequency

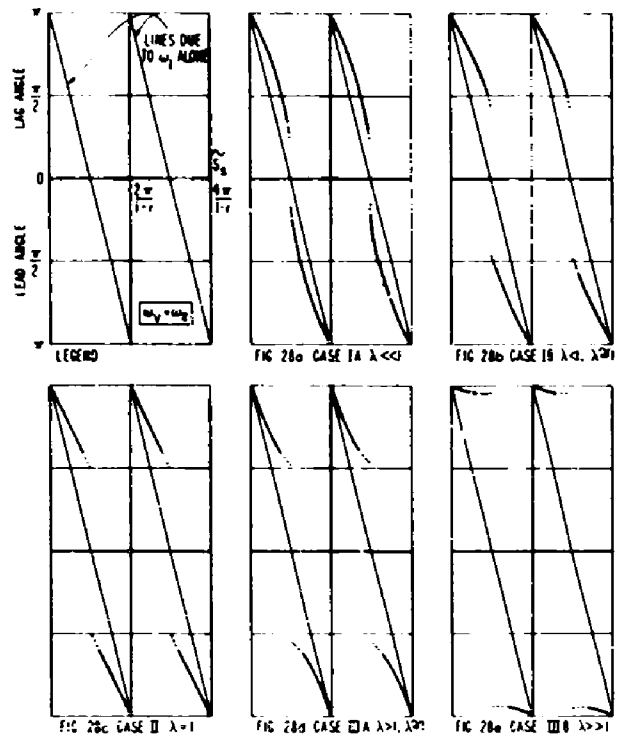


Figure 28 - Change in the pattern of Figure 27 due to a shift of π in the phase of the reference oscillator

APPENDIX II

Comparison of Experimental Observations with Theoretical Predictions for Several Cases of the Superposition of Two Sinusoids

It is of interest to compare the observed appearance of the raster with the form of the trace which is predicted by the theory developed in Appendix I. This Appendix makes such a comparison for several of those cases which are particularly relevant to the sonar applications of the SGI.

An SGI was excited with the sum of two sinusoids of slightly different frequency. The horizontal sweep was turned off, and photographs of the cathode-ray tube face were taken with a strip-film camera.

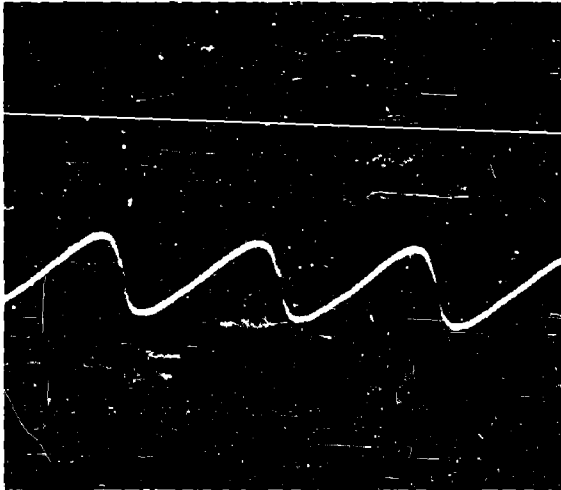
In Figure 29 are shown such photographs for the cases which are encountered when one is detecting one sinusoid in the presence of an interfering sinusoid of slightly different amplitude and frequency. Beside each photograph is repeated the corresponding sketch which has been theoretically predicted.

Figure 30 provides such photographs and corresponding sketches for one of the patterns which can result from nearly equal frequencies but grossly unequal amplitudes, and for one pattern which can result from nearly equal frequencies and almost identical amplitudes.

In Figure 31 are shown photographs and sketches which correspond to patterns which are also frequently observed, namely those for which the reference frequency equals the arithmetic mean of the signal frequencies.

A. Higher frequency is the stronger signal:

(a) Reference frequency is the higher frequency:



24.9 kc at 0 db,
25.0 kc at +3 db.

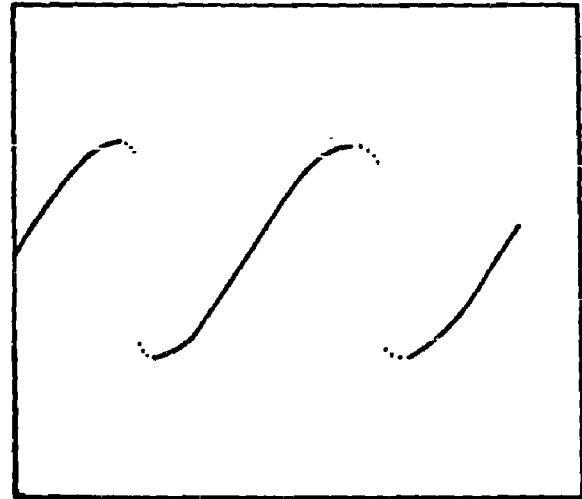


FIG. 7c $A_2 \omega_2 < A_1 \omega_1$, $\frac{A_2 \omega_2}{A_1 \omega_1} \approx 1$
NATURAL PATTERN

(b) Reference frequency is the lower frequency:



24.9 kc at 0 db,
25.0 kc at +3 db.

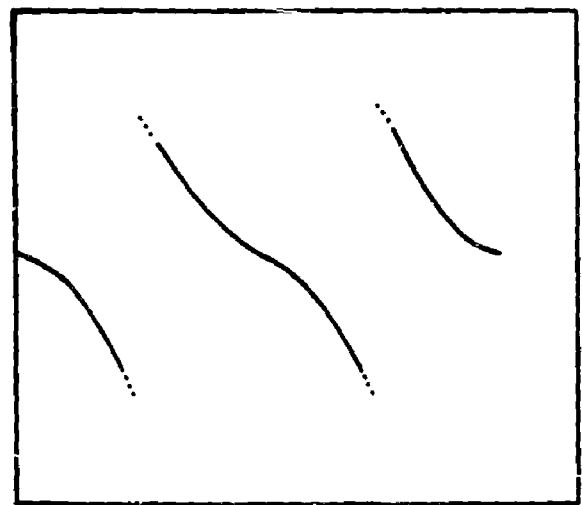
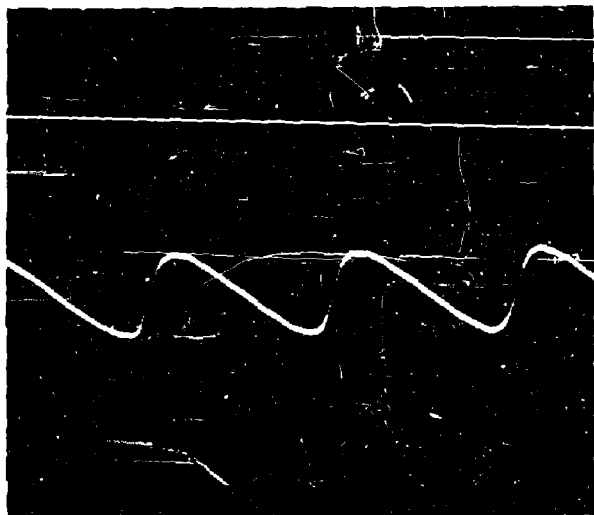


FIG. 8a $A_1 \omega_1 > A_2 \omega_2$, $\frac{A_1 \omega_1}{A_2 \omega_2} \approx 1$

Figure 29 - Photographs and sketches of patterns for slightly different amplitudes and slightly different frequencies

B. Lower frequency is the stronger signal:

(a) Reference frequency is the lower frequency:



25.0 kc at 0 db,
24.9 kc at +3 db.

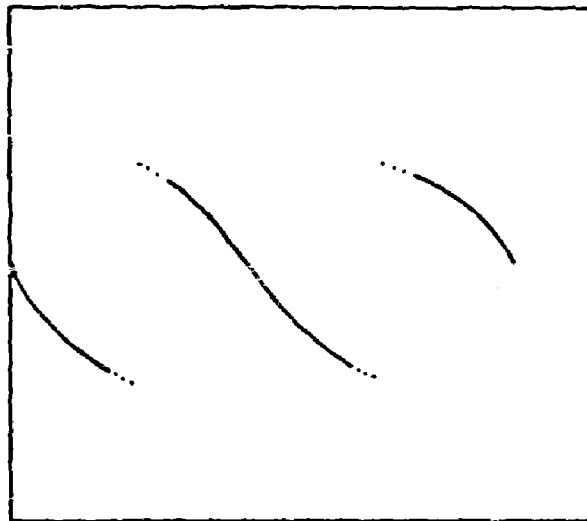


FIG. 8c $A_1 \omega_1 < A_2 \omega_2$, $\frac{A_1 \omega_1}{A_2 \omega_2} \approx 1$

NATURAL PATTERN

(b) Reference frequency is the higher frequency:



25.0 kc at 0 db,
24.9 kc at +3 db.

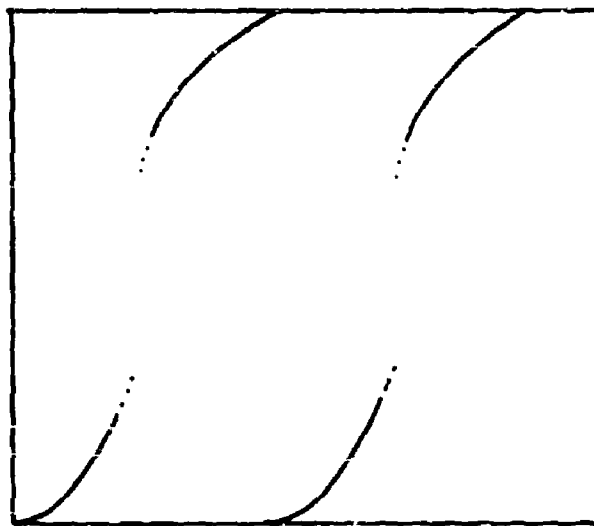


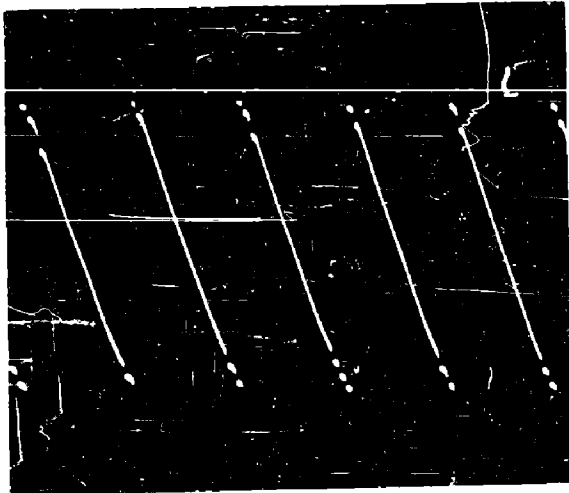
FIG. 7e $A_2 \omega_2 > A_1 \omega_1$, $\frac{A_2 \omega_2}{A_1 \omega_1} \approx 1$

NATURAL PATTERN

Figure 29 (Cont'd) - Photographs and sketches of patterns for slightly different amplitudes and slightly different frequencies

A. Higher frequency is the much stronger signal;

(a) Reference frequency is the lower frequency:



24.9 kc at 0 db,
25.0 kc at +40 db.

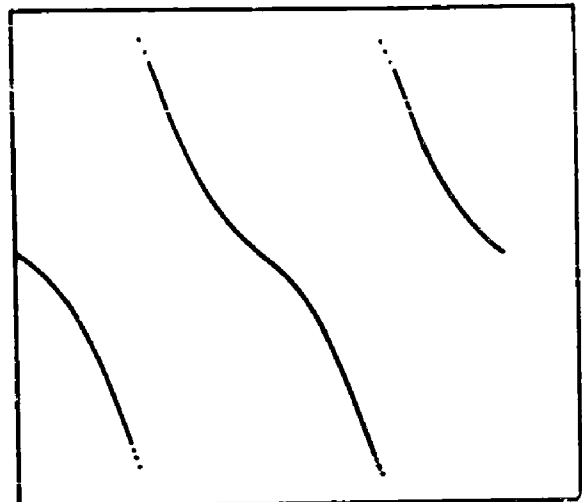
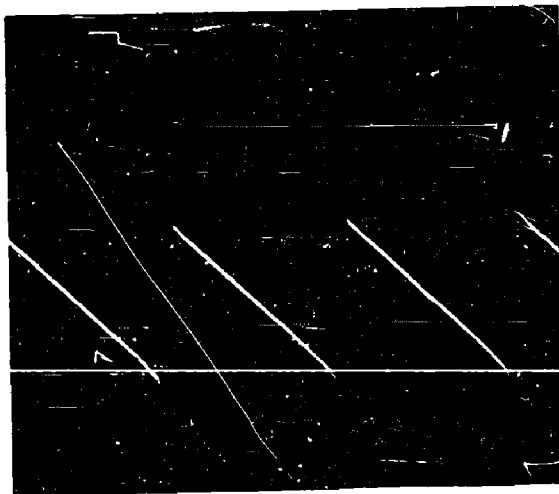


FIG. 8f $A_1 \omega_1 \gg A_2 \omega_2$

B. Higher and lower frequencies have equal amplitudes:

(a) Reference frequency is the lower frequency:



25.0 kc at 0 db,
24.9 kc at 0 db.

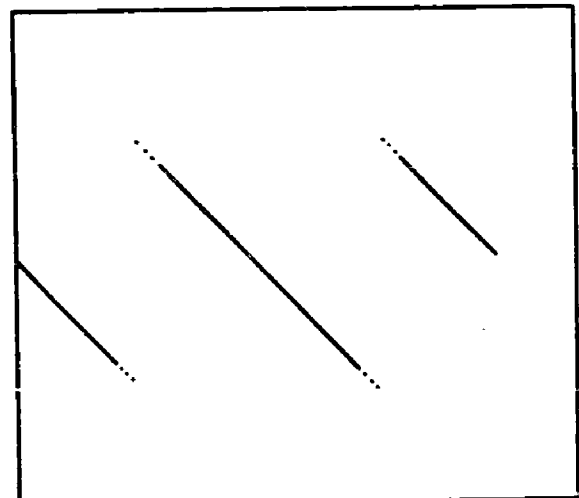
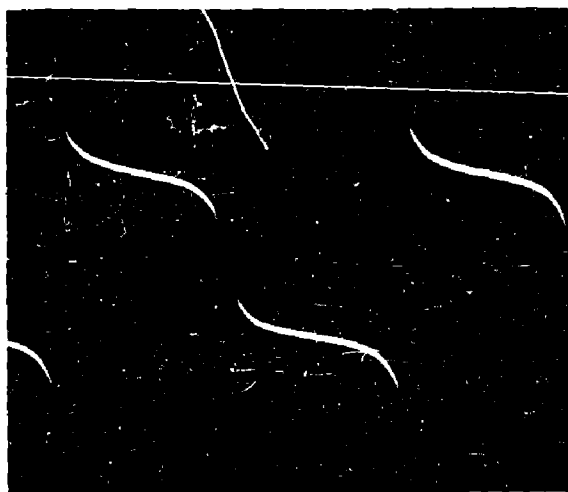


FIG. 8d $A_1 \omega_1 = A_2 \omega_2$

Figure 30 - Photographs and sketches of patterns for grossly unequal, and almost identical, amplitudes

A. Reference frequency equal to the mean of the signal frequencies:

(a) Higher frequency is the stronger signal: *



24.9 kc at 0 db,
25.0 kc at +3 db.

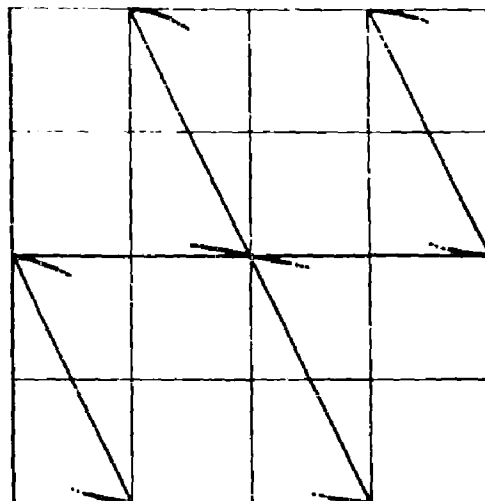
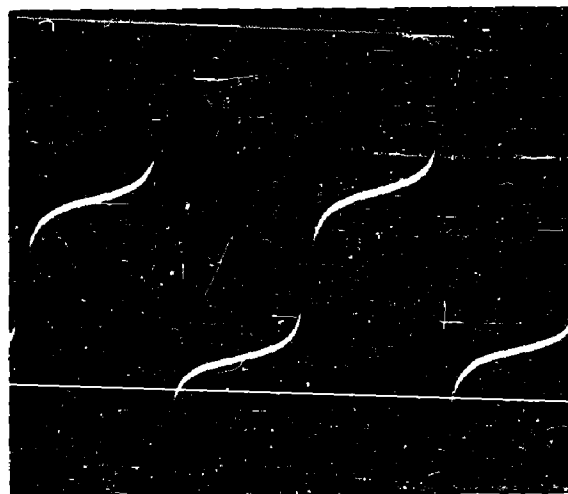


FIG. 26b CASE 10 $\lambda < 1$, $\lambda \approx 1$

(b) Lower frequency is the stronger signal: *



25.0 kc at 0 db,
24.9 kc at +3 db.

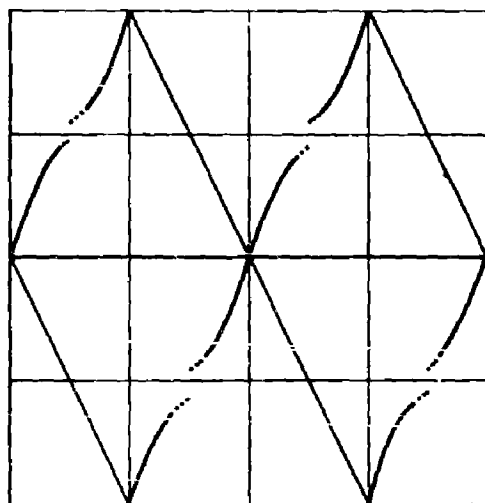


FIG. 26c CASE 11 $\lambda >> 1$

Figure 31 - Photographs and sketches for patterns in which the reference frequency equals the mean of the signal frequencies

*A shift in the phase of the reference oscillator of $\pi/2$ is necessary to cause the photographs and sketches to correspond.

APPENDIX III

Fundamental Equations in Dimensionless Form

Rice* has shown that the expected number** per unit time of positive crossings of a level b by an excitation which is composed of a sinusoidal signal, $A \cos(2\pi f_0 t)$, superimposed upon random noise of the type discussed in Section III.2.2, is (in our notation)

$$N = 2\pi \left(\frac{\int_0^\infty w(f) f^2 df}{\int_0^\infty w(f) df} \right)^{1/2} \phi \left(\frac{b}{\left(\int_0^\infty w(f) df \right)^{1/2}} - \frac{A \cos(2\pi f_0 t)}{\left(\int_0^\infty w(f) df \right)^{1/2}} \right) G \quad (44)$$

where

$$G = \int_0^\infty x \phi \left(x + \frac{A f_0 \sin(2\pi f_0 t)}{\left(\int_0^\infty w(f) f^2 df \right)^{1/2}} \right) dx$$

$w(f)^\dagger$ is the power spectrum of the noise portion of the signal, and ϕ is a function such that, for an arbitrary argument x ,

$$\phi(x) = \frac{1}{\sqrt{2\pi}} e^{-x^2/2}$$

For any particular form of $w(f)$, we are interested in the value of N for three conditions:

*See Rice III, footnote in Section III.2.2.

**The "expected number" per unit time of positive crossings of the level b is a particular average which may be operationally defined in the following way. By "positive crossing" is meant a passage of the excitation amplitude across the level b when the passage is from smaller to larger values. Now, for an arbitrary value of the trigonometric argument, $\psi_0 = 2\pi f_0 t_0$, consider the instants of time corresponding to the values, $n\psi_0$, of the trigonometric argument, where $n = 1, 2, 3, \dots$. Consider also the set of small, equal intervals, Δt in duration, whose midpoints lie at these instants. We label each interval by the subscript appropriate to its midpoint.

Provided the interval Δt is sufficiently short, there will either be one positive crossing of the level b in any specific interval Δt_n ($n = 1, 2, 3, \dots$), or there will be no such crossing. Denote the number of intervals which each contain a positive crossing by N_c .

Then the ratio $N_c / \sum_{n=1}^\infty \Delta t_n$, where the summation is over all values of n (irrespective of the existence of crossings) is the value of the quantity, "expected number of positive crossings per unit time," which corresponds to the arbitrary value ψ_0 .

Rice speaks of this quantity as the "probability of a positive crossing per unit time." Because of the fact that the noise is a stationary time series, Rice's "probability" is equal to our "expected number."

† That is, the power spectrum of the noise at the input to the pulse generator. The functional form of $w(f)$ is hence determined both by the noise spectrum at the input to the transducer, and by the characteristics of the filter which is internal to the device.

N_T - N corresponding to the "top" of the signal: $\cos(2\pi f_0 t) = +1$, $\sin(2\pi f_0 t) = 0$, $A \neq 0$,

N_B - N corresponding to the "bottom" of the signal: $\cos(2\pi f_0 t) = -1$, $\sin(2\pi f_0 t) = 0$,

$A \neq 0$, and

N_N - N corresponding to noise alone: $A = 0$.

For these cases, we have, from Equation (44),

$$\begin{Bmatrix} N_T \\ N_B \\ N_N \end{Bmatrix} = \sqrt{2\pi} \left(\frac{\int_0^\infty w(f) f^2 df}{\int_0^\infty w(f) df} \right)^{1/2} \phi \left(\frac{b}{\left(\int_0^\infty w(f) df \right)^{1/2}} \begin{Bmatrix} - \\ + \\ - \end{Bmatrix} \right) \frac{A}{\left(\int_0^\infty w(f) df \right)^{1/2}} \quad (45)$$

From these three quantities may be obtained those which we use in our analysis, i.e., the number of positive crossings per signal cycle when the sinusoid is absent, C; and the discrimination factor, D. These are, from Equation (45),

$$C = \frac{N_N}{f_0} = \frac{1}{f_0} \left(\frac{\int_0^\infty w(f) f^2 df}{\int_0^\infty w(f) df} \right)^{1/2} e^{-\frac{b^2}{2 \int_0^\infty w(f) df}} \quad (46)$$

and

$$D = \frac{N_T - N_B}{N_T + N_B} = \tanh \frac{bA}{\int_0^\infty w(f) df} \quad (47)$$

As is explained in Section III.2.2, we are treating two cases:

Case I ("white" noise)

$$w(f) = \begin{cases} 0, & f < f_0 - (1 - \theta) a \\ k, & f_0 - (1 - \theta) a \leq f \leq f_0 + \theta a \\ 0, & f_0 + \theta a < f \end{cases} \quad (48)$$

Case II ("6-db" noise)

$$w(f) = \begin{cases} 0, & f < f_0 - (1 - \theta) a \\ h/f^2, & f_0 - (1 - \theta) a \leq f \leq f_0 + \theta a \\ 0, & f_0 + \theta a < f \end{cases} \quad (49)$$

where θ is the fraction of the band above the signal frequency, f_0 .

In Case I, when one carries out the integrations and introduces the variables:

$$\begin{aligned}
 \alpha &= \frac{a}{f_o} \\
 \beta_1 &= \frac{b}{\sqrt{k f_o}} \\
 \sigma_1 &= \frac{A}{\sqrt{k f_o}} \\
 z_1 &= \frac{\beta_1}{\alpha}
 \end{aligned} \tag{50}$$

one finds that

$$C_1^2 = \left[\frac{(1 + \theta \alpha)^3 - (1 - (1 - \theta) \alpha)^3}{3\alpha} \right] e^{-\frac{\beta_1^2}{\alpha}} \tag{51}$$

and

$$D_1 = \tanh(\sigma_1 z_1) \tag{52}$$

Similarly, in Case II, when one introduces the variables:

$$\begin{aligned}
 \alpha &= \frac{a}{f_o} \\
 \beta_2 &= \frac{b}{\sqrt{h/f_o}} \\
 \sigma_2 &= \frac{A}{\sqrt{h/f_o}} \\
 z_2 &= \frac{\beta_2}{\alpha} (1 - (1 - \theta) \alpha) (1 + \theta \alpha)
 \end{aligned} \tag{53}$$

then

$$C_2^2 = [1 - (1 - \theta) \alpha] (1 + \theta \alpha) e^{-\frac{\beta_2^2}{\alpha}} [1 - (1 - \theta) \alpha] (1 + \theta \alpha) \tag{54}$$

and

$$D_2 = \tanh(\sigma_2 z_2) \tag{55}$$

The reader should note that only the variable α is defined in the same way in both Cases I and II. The remaining variables, β , σ , and z , are defined differently in the two cases. In each case, the variable z is defined in such a way that the discrimination function, D , is a monotonically increasing function of z for constant sinusoidal amplitude, constant noise spectrum, and constant signal frequency. This is done for analytical convenience. The quantities β and σ are chosen, like α , to be nondimensional. Because of the different nature of the noise spectrum in the two cases, their definitions are then necessarily different.

APPENDIX IV

Optimization with Respect to θ

This appendix is devoted to a proof of the following proposition:

Theorem—If the noise power spectrum is a nonincreasing function of frequency (and the other conditions of the theory as described in Section III.2 are maintained), then $\theta = 1$ is an optimum condition.

Introducing the notation:

$$\psi(a, \theta) = \int_{f_0 - (1-\theta)a}^{f_0 + \theta a} w(f) f_0^2 df \quad (56)$$

and

$$\psi''(a, \theta) = \int_{f_0 - (1-\theta)a}^{f_0 + \theta a} w(f) f^2 df \quad (57)$$

the basic equations to be treated (Appendix III) take the form

$$C^{*2} = \frac{\psi''}{\psi} \exp \left\{ - (bf_0)^2 / \psi \right\}, \quad (58)$$

$$z = bf_0^2 / \psi. \quad (59)$$

In particular, z is to be maximized subject to the constraint in Equation (58). As described in Section III.3, this may be accomplished by projecting the space curve represented by Equations (58) and (59) in the zab -space into any particular plane in this space which contains the z -axis. The maximum point on this projected curve represents a solution to the problem.

In particular, we may project into the za -plane by eliminating b between Equations (58) and (59), obtaining

$$C^{*2} = \frac{\psi''}{\psi} \exp \left\{ - \zeta \psi \right\} \quad (60)$$

where

$$\zeta = (z/f_0)^2 \quad (61)$$

If we can show that at any value of α , and for fixed C^* , the value of ζ defined by Equation (60) increases with θ , the theorem is proved. For, in this event, if the highest point on

the particular curve $z(\alpha, \theta_1)$ is found, it is not a maximum with respect to θ because the value of z can always be increased by holding α fixed and letting $\theta > \theta_1$.

From Equation (60), we have

$$\frac{\partial \zeta}{\partial \theta} = \frac{1}{\psi} \left[\frac{\psi''_{\theta}}{\psi''} - \frac{\psi_{\theta}}{\psi} (1 + \zeta \psi) \right] \quad (62)$$

the subscript θ denoting partial derivative with respect to θ . Let us use subscripts U and L to denote values at the upper and lower limits of integration of the integrals of Equations (56) and (57). Then

$$\psi_{\theta} = f_c^2 a(w_U - w_L) \quad (63)$$

and

$$\psi''_{\theta} = a \left[(wf^2)_U - (wf^2)_L \right] \quad (64)$$

By the terms of the theorem, $w_U \leq w_L$; so $\psi_{\theta} \leq 0$. Using this, we may rewrite Equation (62) as:

$$\frac{\partial \zeta}{\partial \theta} = \frac{1}{\psi} \left[\frac{\psi''_{\theta}}{\psi''} + \frac{|\psi_{\theta}|}{\psi} (1 + \zeta \psi) \right] \quad (65)$$

Recall that from their definitions, ψ , ψ'' , and ζ are all positive.

Two cases now arise. First, if $\psi''_{\theta} > 0$, $\partial \zeta / \partial \theta > 0$ and the theorem is proved. Second, if $\psi''_{\theta} < 0$, then a sufficient condition for the truth of the theorem is

$$\frac{|\psi''_{\theta}|}{\psi''} \leq \frac{|\psi_{\theta}|}{\psi} \quad (66)$$

It is clear from Equation (60), that in order to have a solution of the problem at all, $\psi''/\psi \geq C^2$, whence $\psi'' \geq \psi$. Hence,

$$|\psi''_{\theta}|/\psi'' \leq |\psi_{\theta}|/\psi \quad (67)$$

Moreover, it can be seen that if $\psi''_{\theta} < 0$, then $(wf_o^2)_L \geq (wf^2)_L \geq (wf^2)_U \geq (wf_o^2)_U$

whence

$$|\psi''_{\theta}| = a \left[(wf^2)_L - (wf^2)_U \right] \leq a \left[(wf_o^2)_L - (wf_o^2)_U \right] = |\psi_{\theta}| \quad (68)$$

From Equations (67) and (68) then, $|\psi''_{\theta}|/\psi'' \leq |\psi_{\theta}|/\psi$, and the theorem is proved.

APPENDIX V

White Noise

The problem is to find those values of (α, β) which maximize D_1 for a specified C_1^* and a fixed σ_1 . Such values will be called the optimum values (α_m, β_m) .^{*} It will be shown that with $C^* > 1$, there exist unique optimum values for α and β . The corresponding value of z , and therefore of D , is a stationary maximum.

The equations to be satisfied are:

$$C^{*2} = \left[\frac{(1 + \alpha)^3 - 1}{3\alpha} \right] e^{-\beta^2/\alpha}, \quad (69)$$

$$z = \beta/\alpha. \quad (70)$$

In this case, one can project the curve of intersection of these surfaces into the particular radial plane $\phi = 0$ (i.e. the $z\alpha$ -plane) by eliminating β . One obtains

$$z^2 = \frac{1}{\alpha} \ln \left[\frac{3 + 3\alpha + \alpha^2}{3C^{*2}} \right] \quad (71)$$

The value α_m , which makes z a maximum in this plane, clearly corresponds to a maximum of the original space curve. Equation (71) defines a real curve in the $z\alpha$ -plane for

$$\alpha > \frac{2}{3} \left[\sqrt{1 + \frac{16}{3}(C^{*2} - 1)} - 1 \right] = \alpha_0 \quad (72)$$

with α_0 defined by the last equation.

Theorem—The curve in the $z\alpha$ -plane represented by Equation (71) has exactly one stationary maximum.

Proof—There is at least one stationary maximum, since $z(\alpha_0) = z(\infty) = 0$ and $z(\alpha) \geq 0$, $\alpha_0 \leq \alpha$, both $z(\alpha)$ and $dz/d\alpha$ being continuous for $\alpha > \alpha_0$. Clearly, any stationary maximum satisfies

$$\frac{\alpha(3 + 2\alpha)}{3 + 3\alpha + \alpha^2} = \ln \left[\frac{3 + 3\alpha + \alpha^2}{3C^{*2}} \right] \quad (73)$$

We show that this equation has at most one solution, $\alpha_m > \alpha_0$.

The right hand side, $R(\alpha)$, and left hand side, $L(\alpha)$, of Equation (73) are equal at any solution α_m .

^{*}Throughout this appendix and the next, the subscripts 1 and 2 will be omitted for brevity. It is to be understood that the variables treated in these appendices are those defined with subscripts in Equations (50) and (53) respectively.

Now,

$$\frac{dL(\alpha)}{d\alpha} \bigg/ \frac{dR(\alpha)}{d\alpha} = 1 - \frac{\alpha(3 + 6\alpha + 2\alpha^2)}{(3 + 2\alpha)(3 + 3\alpha + \alpha^2)} < 1,$$

or the slope of the right hand side exceeds the slope of the left hand side at every value of α . Thus, if $R(\alpha)$ and $L(\alpha)$ have a common value at α_m , they cannot become equal again at any $\alpha > \alpha_m$. Moreover, α_0 is not a solution. This means that there is at most one solution $\alpha_m > \alpha_0$.

For the case of white noise, one concludes that the optimum α_m is the unique solution of Equation (73). The value z_m can be found from Equation (71), knowing α_m , and the corresponding β_m from Equation (70). Both optimum parameters (α_m, β_m) depend upon the value assigned to C^* .

APPENDIX VI

Six-db Noise

The problem is to choose values (α_m, β_m) which maximize z , subject to the constraint $C(\alpha, \beta) = C^*$, for the case where:

$$z = \beta(1 + \alpha)/\alpha \quad (74)$$

and

$$C^{*2} = (1 + \alpha) \exp \left\{ -\beta^2(1 + \alpha)/\alpha \right\} \quad (75)$$

In terms of polar coordinates defined by Equation (26), these two equations take the form

$$C^{*2} \tan \phi = z \exp \left\{ -\rho z \sin \phi \right\} \quad (76)$$

and

$$z = \tan \phi (1 + \rho \cos \phi) \quad (77)$$

The general features of the curves defined in a radial plane $\phi = \text{constant}$ by the last two equations are shown in Figures 32 and 33. It is clear from the figures that if ϕ is sufficiently small, i.e., $C^{*2} e \tan \phi < 1$,

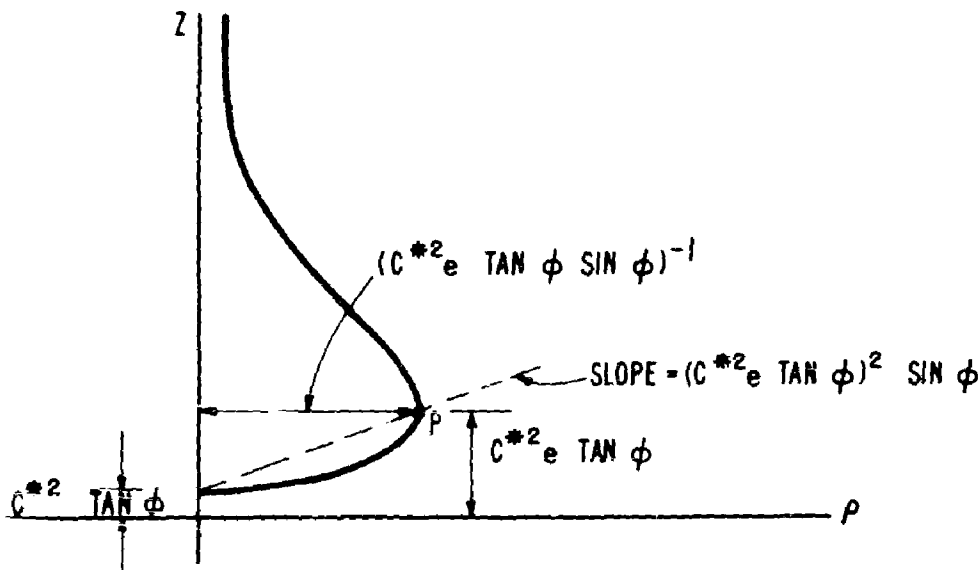


Figure 32 - Curve defined by Equation 76

there is exactly one solution, z^* , of the two equations which has a z -value above the point P in Figure 32.

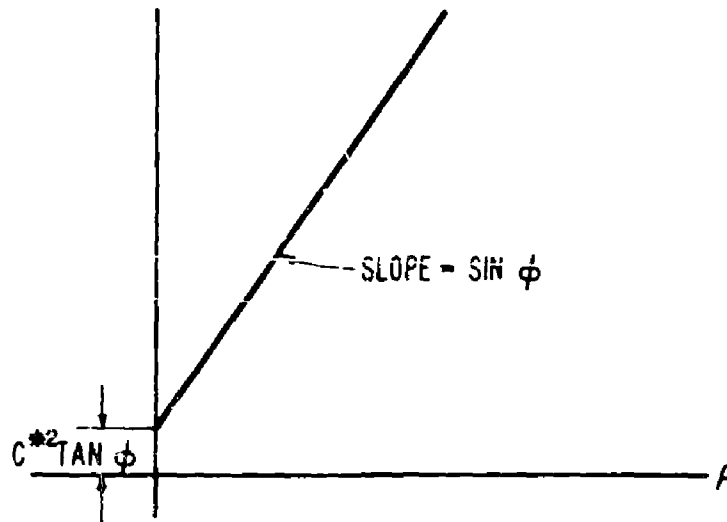


Figure 33 - Curve defined by Equation 77

The z -value of this solution satisfies the single equation

$$C^2 \tan \phi = z \exp \{z(\tan \phi - z)\} \quad (78)$$

It will now be shown that as ϕ is reduced toward zero, beyond the point at which the solution z^* appears uniquely on the upper branch of the curve of Figure 32, the solution z^* increases indefinitely.

Theorem—For any fixed C^* , the optimum solution $z_m(C^*)$ corresponds to the smallest value of ϕ permitted by physical considerations.

Proof—From Equation (78),

$$\frac{dz^*}{d\phi} = \frac{z^* \sec \phi}{\sin \phi} \left[\frac{1 - z^* \tan \phi}{1 - z^*(2z^* - \tan \phi)} \right]$$

Moreover, the same equation gives

$$z^*(2z^* - \tan \phi) - 1 = (z^*)^2 + \ln \left[\frac{z^*}{C^2 e \tan \phi} \right]$$

Since z^* is above point P, the argument of the logarithm exceeds unity and there is no question that $z^*(2z^* - \tan \phi) - 1 > 0$. Therefore, $\text{sgn } dz^*/d\phi = -\text{sgn}(1 - z^* \tan \phi)$. Now rewrite Equation (78) as

$$C^2 z^* \tan \phi e^{-z^* \tan \phi} = (z^*)^2 e^{-(z^*)^2}$$

The right and left hand sides (RHS and LHS) of this equation appear graphically as shown in Figure 34. It is clear that their intersection, which gives the solution z^* , satisfies $z^* < \cot \phi$ or $z^* \tan \phi < 1$. Hence $\text{sgn } dz^*/d\phi = -1$. Since the solution z^* thus increases with decreasing ϕ , the value of ϕ should be taken as small as physical considerations permit in finding an optimum z_m .

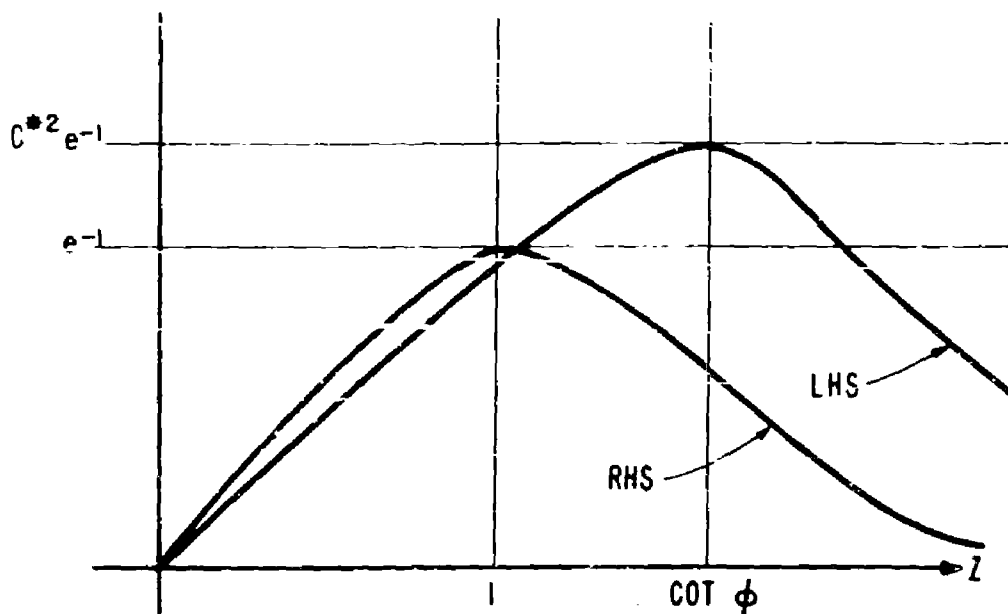


Figure 34 - Curves defined by Equation 78

One may be led to investigate the behavior of the possible intersection of the curves of Equations (76) and (77) which lies below the point P. This intersection is of no consequence, however, since it can be shown to disappear as $\phi = \pi/4$, and for $\phi < \pi/4$ it lies below $C^2 e$.

Suppose that there is an upper bound α^* to the realizable bandwidth. This restricts the smallness of ϕ , and immediately gives $\alpha_m = \alpha^*$. Returning to Equation (75), the corresponding optimum bias is

$$\beta_m = \left[\left(\frac{\alpha^*}{1 + \alpha^*} \right) \ln \left(\frac{1 + \alpha^*}{C^2} \right) \right]^{1/2} \quad (79)$$

The optimum z_m is easily obtained from Equation (74).

A word of interpretation with regard to the form of the last equation is necessary. Clearly, it is nonsense if $C^2 > 1 + \alpha^*$. This means simply that if the bandwidth of the system is too low, the number of background spots per cycle required by the specified C^* cannot be realized. In such a case, one must either content himself with a lower background of spots, or must find a way to increase the passband of the system.

APPENDIX VII

Notation

A: amplitude of a sinusoid
 A: ability function
 C: crossings per signal cycle
 D: relative intensity of spots
 H: raster height
 K: positive integer
 L: positive integer
 M: positive integer
 N: number of spots
 P: undetermined multiplier
 Q: undetermined multiplier
 R: range rate
 S: slope of line on raster
 T: period
 V: speed
 W: raster width
 X: increment in displacement

 a: width of passband
 b: bias level
 c: velocity of sound
 f: frequency
 h: constant in the 6-db-per-octave noise spectrum
 k: constant in the white noise spectrum
 n: positive integer
 o: positive integer
 q: positive integer
 r: frequency ratio
 s: ratio of positive integers
 t: time
 w: noise spectrum
 x: horizontal coordinate on raster
 y: vertical coordinate on raster
 z: dimensionless function of bias, bandwidth, and θ .

 α : dimensionless width of passband
 β : dimensionless bias level
 γ : angle made with the horizontal by a line of spots on raster
 ζ : normalized z
 θ : fraction of passband above operating frequency
 λ : ratio of maximum slopes of two sinusoids
 ξ : sinusoidal function of time
 ρ : radius vector
 σ : dimensionless signal to noise ratio
 τ : dimensionless trigonometric argument
 ϕ : phase angle of a sinusoid
 ϕ : polar angle; error function
 ψ : moments over w
 ψ : phase angle; trigonometric argument
 ω : circular frequency

VERTICAL SHEET FREQUENCY EQUAL TO HIGHER COMPONENT FREQUENCY

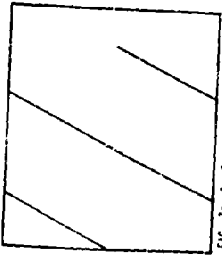
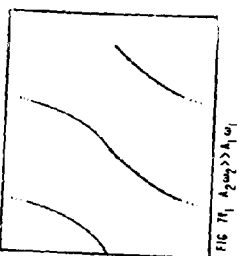
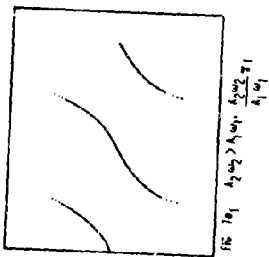
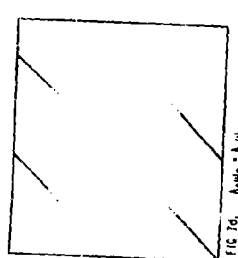
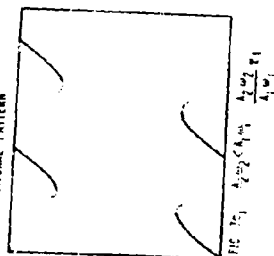
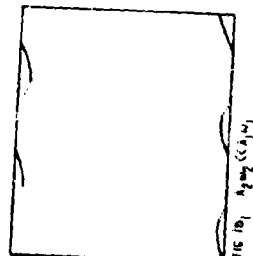
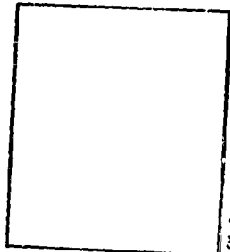
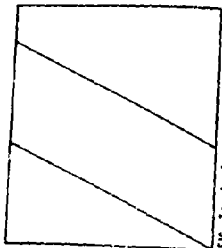
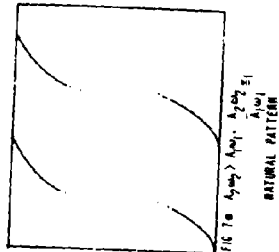
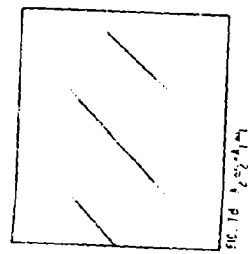
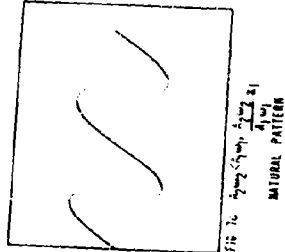
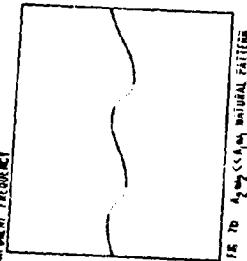
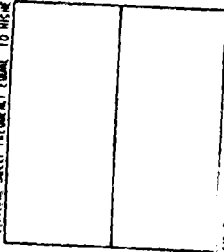


Figure 7 - Patterns when reference frequency equals higher frequency

VERTICAL SHEET FREQUENCY EQUAL TO THE LOWER COMPONENT FREQUENCY

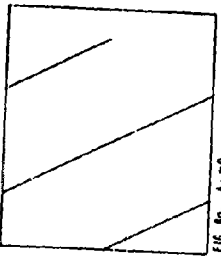
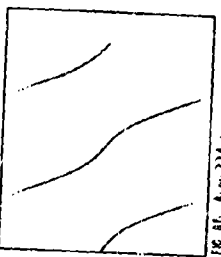
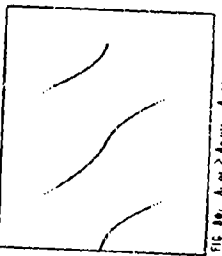
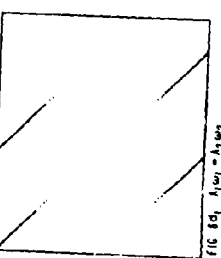
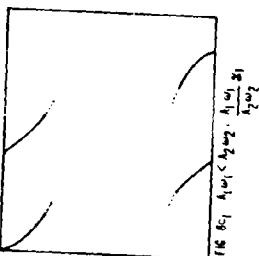
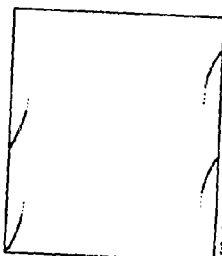
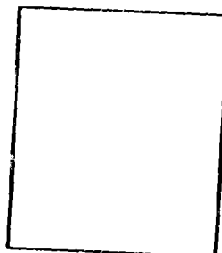
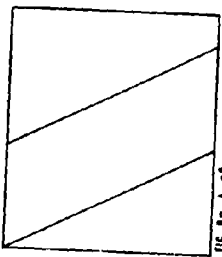
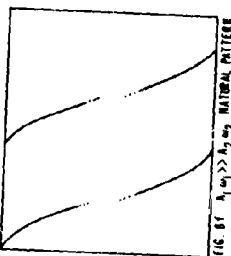
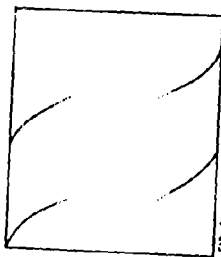
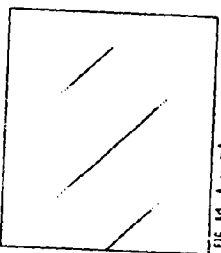
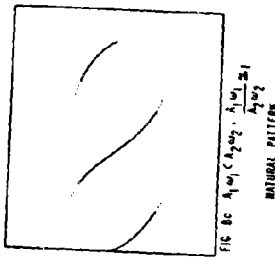
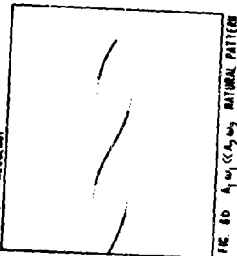
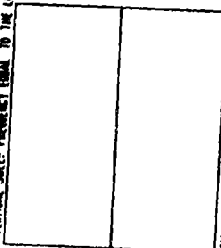


Figure 8 - Patterns when reference frequency equals lower frequency

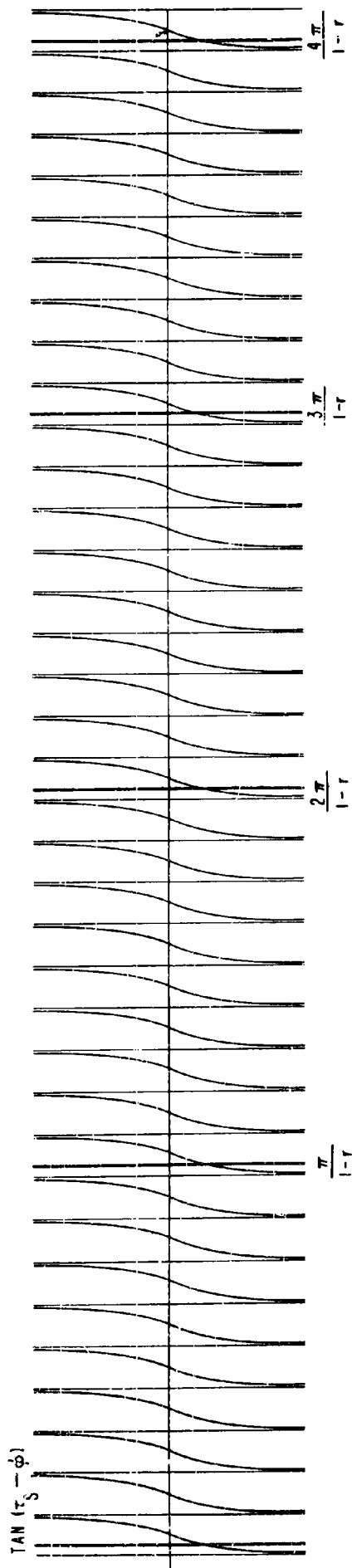


Figure 16 - $\text{TAN}(\tau_s - \phi)$ versus r

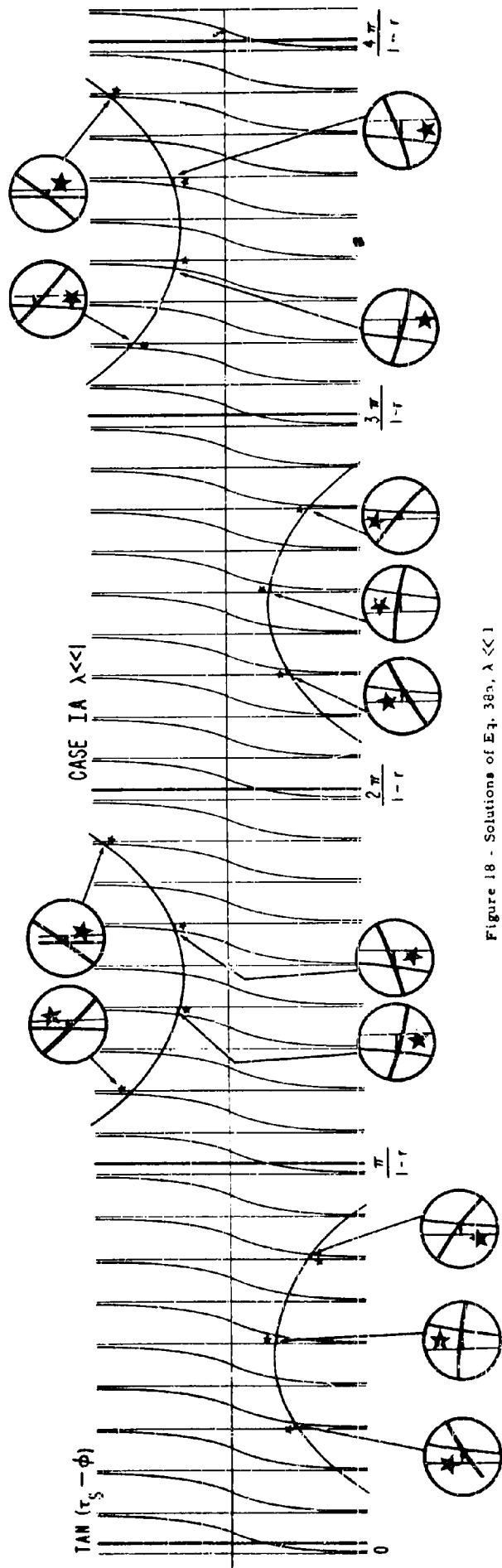


Figure 18 - Solutions of Eq. 38a, $\lambda \ll 1$

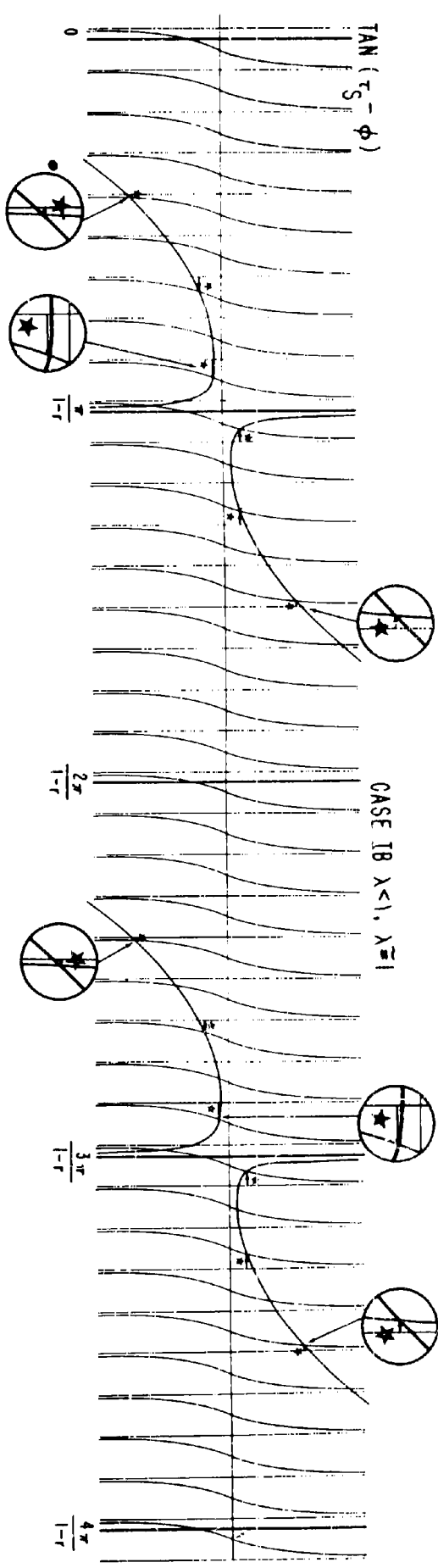


Figure 19 - Solutions of Eq. 38a, $\lambda < 1$, $\lambda \approx 1$

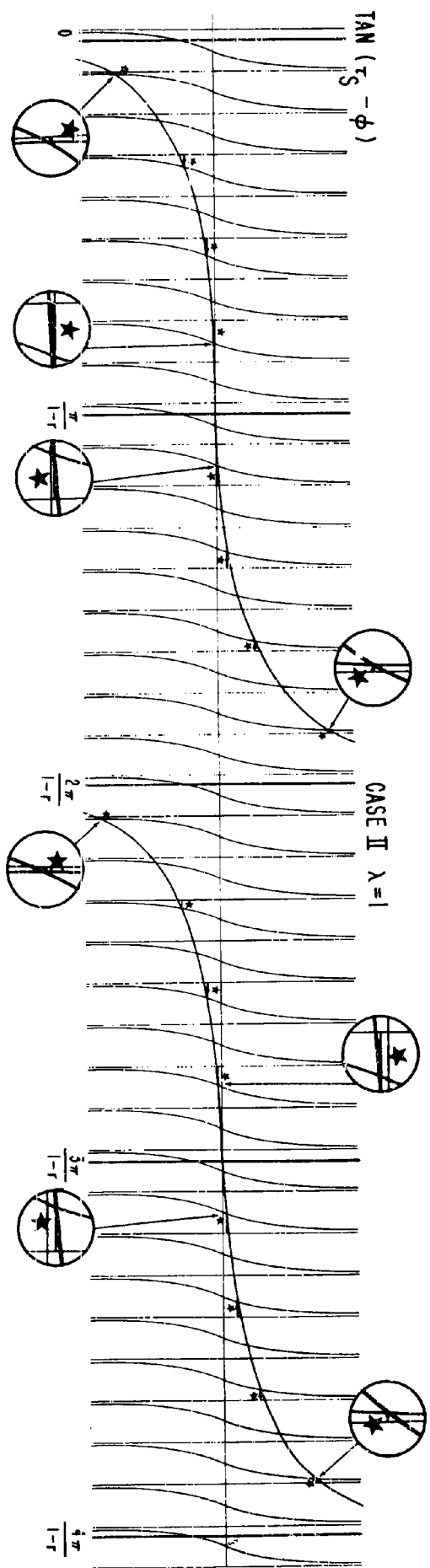


Figure 20 - Solutions of Eq. 38a, $\lambda = 1$

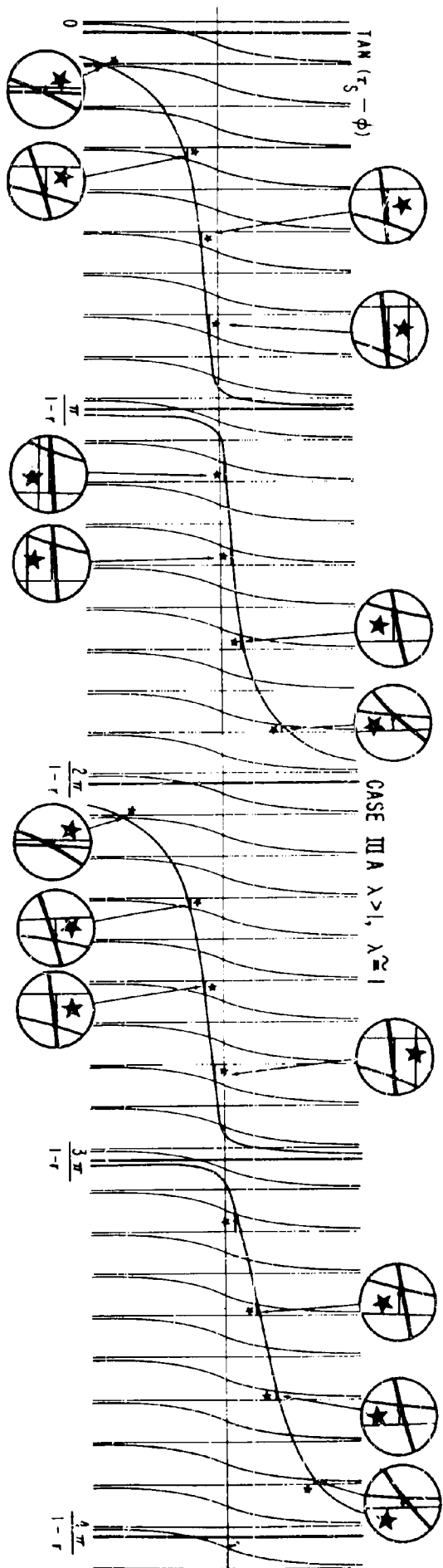


Figure 21 - Solutions of Eq. 38a, $\lambda > 1$, $\lambda \approx 1$

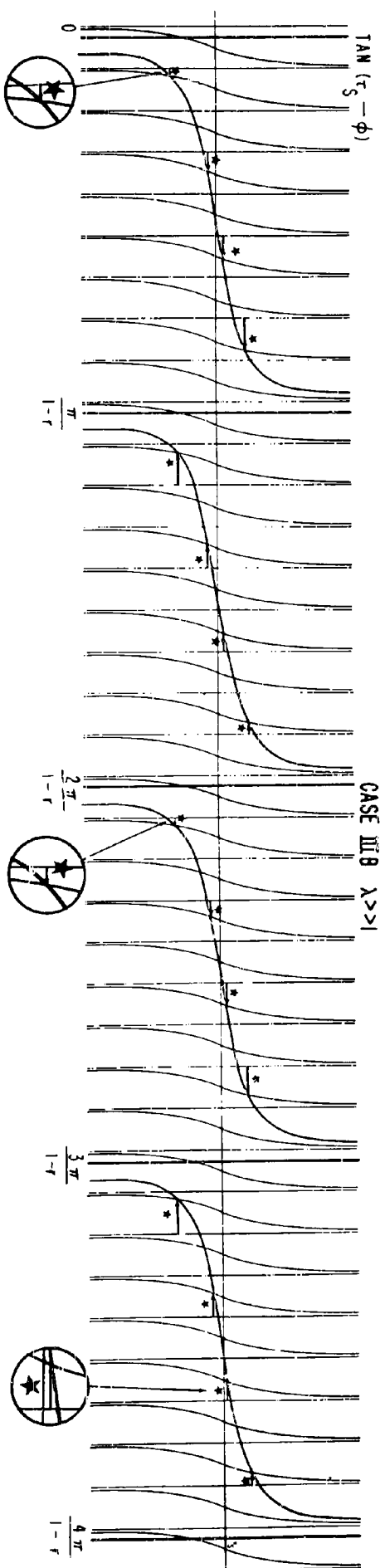


Figure 22 - Solutions of Eq. 38a, $\lambda \gg 1$

DETACHABLE ABSTRACT CARDS

These abstract cards are inserted in NRL Reports for the convenience of librarians and others who need to maintain an information index.

Detached cards are subject to the same Security Regulations as the parent document and a record of their location should be made on the inside of the back cover of the parent document.

<p style="text-align: center;">SECRET SECURITY INFORMATION</p> <p>Naval Research Laboratory. Report 4199. SOME THEORETICAL ASPECTS OF THE SONAR GRAPHIC INDICATOR, by R. E. Roberson, S. P. Thompson and H. M. Trent. 69 pp. & figs., October 12, 1953.</p> <p>This report deals with some of the more important theoretical aspects of one of the Navy's newest sonar devices, the Sonar Graphic Indicator.</p> <p>Emphasis in Part I is upon the visual patterns which are produced by the device in response to a periodic signal, and to the important tactical uses to which these patterns may be put.</p> <p>Parts II and III concern the device's ability to perform in the presence of reverberations and random noise.</p> <p style="text-align: right;">(Over) SECRET</p>	<p style="text-align: center;">SECRET SECURITY INFORMATION</p> <p>Naval Research Laboratory. Report 4196. SOME THEORETICAL ASPECTS OF THE SONAR GRAPHIC INDICATOR, by R. E. Roberson, S. P. Thompson and H. M. Trent. 69 pp. & figs., October 12, 1953.</p> <p>This report deals with some of the more important theoretical aspects of one of the Navy's newest sonar devices, the Sonar Graphic Indicator.</p> <p>Emphasis in Part I is upon the visual patterns which are produced by the device in response to a periodic signal, and to the important tactical uses to which these patterns may be put.</p> <p>Parts II and III concern the device's ability to perform in the presence of reverberations and random noise.</p> <p style="text-align: right;">(Over) SECRET</p>	<p>I. Sonar Graphic Indicator - Development</p> <p>II. R. E. Roberson</p> <p>III. S. P. Thompson</p> <p>IV. H. M. Trent</p>	<p>I. Sonar Graphic Indicator - Development</p> <p>II. R. E. Roberson</p> <p>III. S. P. Thompson</p> <p>IV. H. M. Trent</p>
<p style="text-align: center;">SECRET SECURITY INFORMATION</p> <p>Naval Research Laboratory. Report 4199. SOME THEORETICAL ASPECTS OF THE SONAR GRAPHIC INDICATOR, by R. E. Roberson, S. P. Thompson and H. M. Trent. 69 pp. & figs., October 12, 1953.</p> <p>This report deals with some of the more important theoretical aspects of one of the Navy's newest sonar devices, the Sonar Graphic Indicator.</p> <p>Emphasis in Part I is upon the visual patterns which are produced by the device in response to a periodic signal, and to the important tactical uses to which these patterns may be put.</p> <p>Parts II and III concern the device's ability to perform in the presence of reverberations and random noise.</p> <p style="text-align: right;">(Over) SECRET</p>	<p style="text-align: center;">SECRET SECURITY INFORMATION</p> <p>Naval Research Laboratory. Report 4196. SOME THEORETICAL ASPECTS OF THE SONAR GRAPHIC INDICATOR, by R. E. Roberson, S. P. Thompson and H. M. Trent. 69 pp. & figs., October 12, 1953.</p> <p>This report deals with some of the more important theoretical aspects of one of the Navy's newest sonar devices, the Sonar Graphic Indicator.</p> <p>Emphasis in Part I is upon the visual patterns which are produced by the device in response to a periodic signal, and to the important tactical uses to which these patterns may be put.</p> <p>Parts II and III concern the device's ability to perform in the presence of reverberations and random noise.</p> <p style="text-align: right;">(Over) SECRET</p>	<p>I. Sonar Graphic Indicator - Development</p> <p>II. R. E. Roberson</p> <p>III. S. P. Thompson</p> <p>IV. H. M. Trent</p>	<p>I. Sonar Graphic Indicator - Development</p> <p>II. R. E. Roberson</p> <p>III. S. P. Thompson</p> <p>IV. H. M. Trent</p>

Its action in discriminating against reverberations is studied in Part II by considering in detail the patterns which are produced by a superposition of two sinusoids of slightly different frequency.

In Part III is considered the problem of choosing the device's design parameters in such a manner that the operator can best detect a periodic signal in the presence of random noise. Information regarding the optimum values of the bias, bandwidth, and nominal operating frequency is deduced on the basis of plausible but admittedly assumed notions about the observer's psychology with respect to visual perception. Particular attention is paid to noise spectrums which are "white," or which fall at 6 db per octave

SECRET

SECRET

Its action in discriminating against reverberations is studied in Part II by considering in detail the patterns which are produced by a superposition of two sinusoids of slightly different frequency.

In Part III is considered the problem of choosing the device's design parameters in such a manner that the operator can best detect a periodic signal in the presence of random noise. Information regarding the optimum values of the bias, bandwidth, and nominal operating frequency is deduced on the basis of plausible but admittedly assumed notions about the observer's psychology with respect to visual perception. Particular attention is paid to noise spectrums which are "white," or which fall at 6 db per octave

SECRET

Its action in discriminating against reverberations is studied in Part II by considering in detail the patterns which are produced by a superposition of two sinusoids of slightly different frequency.

In Part III is considered the problem of choosing the device's design parameters in such a manner that the operator can best detect a periodic signal in the presence of random noise. Information regarding the optimum values of the bias, bandwidth, and nominal operating frequency is deduced on the basis of plausible but admittedly assumed notions about the observer's psychology with respect to visual perception. Particular attention is paid to noise spectrums which are "white," or which fall at 6 db per octave

Its action in discriminating against reverberations is studied in Part II by considering in detail the patterns which are produced by a superposition of two sinusoids of slightly different frequency.

In Part III is considered the problem of choosing the device's design parameters in such a manner that the operator can best detect a periodic signal in the presence of random noise. Information regarding the optimum values of the bias, bandwidth, and nominal operating frequency is deduced on the basis of plausible but admittedly assumed notions about the observer's psychology with respect to visual perception. Particular attention is paid to noise spectrums which are "white," or which fall at 6 db per octave

SECRET

CLASSIFICATION CHANGED

AD

FROM SECRET TO CONFIDENTIAL

30443

ON

By authority of

List No. 49

Specify Authority Being Used

This action was rendered by

Arthur L. Creech OSA

Name in full

Date

Document Service Center, ASTIA

UNITED STATES GOVERNMENT
memorandum

7103/111

DATE: 22 October 1996

FROM: Burton G. Hurdle (Code 7103)

SUBJECT: REVIEW OF REF. (a) FOR DECLASSIFICATION

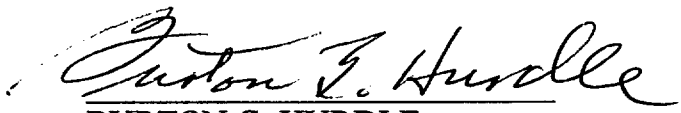
TO: Code 1221.1

VIA: Code 7100

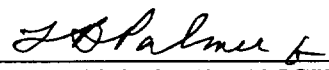
AD-030 443

REF: (a) NRL Confidential Report #4199 by R.E. Robinson et al, Oct. 12, 1953 (U)
(b) NRL ltr 1570-476/55 of 28 July 1955

1. Reference (a) is a theoretical investigation of the basics underlying the sonar graphic indicator. The sonar graphic indicator is a method of measuring the phase of a sonar signal on a cycle-to-cycle basis and displaying it on a cathode ray screen. The phase pattern of the signal is used for classification and for measuring the speed, via the Doppler shift, and range of the target.
2. The AN/BQA-3 was the practical utilization of this technology. The AN-BQA-3 has not been in service in submarines for at least ten years, this technology being superseded.
3. Reference (a) was declassified to Confidential by reference (b).
4. Based on the above, it is recommended that reference (a) be declassified with no restrictions.


BURTON G. HURDLE
Acoustics Division

CONCUR:


EDWARD R. FRANCHI
Superintendent
Acoustics Division

10/22/96
Date

